Tectonophysics 658 (2015) 169–185

Contents lists available at ScienceDirect

Tectonophysics

journal homepage: www.elsevier.com/locate/tecto

Modelling the coupling between salt kinematics and subsidence evolution: Inferences for the Miocene evolution of the Transylvanian Basin

Marius Tilita [a,b,*], Magdalena Scheck-Wenderoth [c,d], Liviu Matenco [a], Sierd Cloetingh [a]

[a] Utrecht University, Faculty of Geosciences, Department of Earth Sciences, Budapestlaan 6, 3584CD, Utrecht, The Netherlands
[b] Repsol Exploración S.A., Mendez Álvaro 44, 28045, Madrid, Spain
[c] Helmholtz Centre Potsdam-GFZ German Research Centre for Geosciences, Telegrafenberg, D-14473 Potsdam, Germany
[d] RWTH Aachen, Germany

ARTICLE INFO

Article history:
Received 16 February 2015
Received in revised form 15 July 2015
Accepted 27 July 2015
Available online 8 August 2015

Keywords:
Salt kinematics
Basin evolution
Intraplate stresses
Transylvanian Basin

ABSTRACT

Large-scale diapiric salt movements affect the architecture of sedimentary basins and often prevent the understanding of their mechanics by hiding or distorting subsidence patterns. One good example is the evolution of the Transylvanian Basin, which formed during Miocene times in an area located in between the rapid slab rollback and continental collision recorded at the exterior of the Carpathians and the extension of the neighbouring Pannonian Basin. In the absence of major genetic fault systems, quantifying these external tectonic forcing factors requires an accurate reconstruction of subsidence evolution. Having the advent of a detailed 3D geometrical model of the Transylvanian Basin, we apply a 3D numerical modelling technique that couples salt re-distribution and subsidence evolution to quantify and understand the basin kinematics and vertical motions. Two techniques, backward and forward modelling are coupled in order to discriminate between salt migration driven by overburden and the influence of external tectonic forcing factors. The results show that salt kinematics was more complex than simple unidirectional migration, suggesting the existence of areas with significant subsidence hidden by the inward salt migration and areas with apparent large subsidence that are in reality artefacts of outwards salt migration. Additionally, the results suggest that parts of the basin have been successively affected by in- and out-ward salt migration events, an effect of localising subsidence and overburden. Furthermore, accelerated moments of salt migration took place during the main Miocene contraction events recorded at the exterior of the Carpathians, demonstrating that salt migration is enhanced by intraplate stresses. Our study also infers that the subsidence of the Transylvanian Basin is the result of the superposition of the contraction at the exterior of the orogenic chain and the back-arc extension.

1. Introduction

The evolution of sedimentary basins reflects the close feedback between deep and near-surface processes, as well as the interaction between erosion of the source areas and deposition in the nearby sinks (e.g., Cloetingh et al., 2013; Matenco and Andriessen, 2013). One major factor affecting their internal geometry is salt diapirism that deforms the overlying depositional sequence and is superposed over first order basin formation structures. Understanding the interplay between salt kinematics and tectonic subsidence commonly requires a reasonably detailed subsurface image combined with modelling studies (e.g., Brun and Fort, 2011; McClay et al., 2004; Nagihara et al., 1992; Poliakov et al., 1993; Smit et al., 2008). This understanding is of major importance for deriving resource plays, such as hydrocarbon or geothermal (e.g., Beglinger et al., 2012; Cloetingh et al., 2010; Corver et al., 2011).

Observational studies infer that salt kinematics in basins without significant tectonic activity is generally driven by the geometry of overlying sediments, original deposition and geothermal distribution (e.g., Petersen and Lerche, 1995; Warsitzka et al., 2013). Modelling studies indicate that the presence of significant tectonic stress is essential for the formation of large and exaggerated diapiric structures, which are relevant for understanding regional basin evolution (e.g., Daudré and Cloetingh, 1994; Hecht et al., 2003; Jenyon, 1986; Krézsek et al., 2007). Basins where salt was deposited during the early stages of evolution and was not significantly deformed afterwards facilitate an easier understanding of its kinematics and of the constant interplay of subsidence–salt migration. This is the case of the North German basin, North Sea or the western Atlantic passive continental margin (e.g., Beglinger et al., 2012; Scheck and Bayer, 1999; Thomsen and

* Corresponding author at: Repsol Exploración S.A., Mendez Álvaro 44, 28045, Madrid, Spain.
E-mail address: marius.tilita@gmail.com (M. Tilita).

http://dx.doi.org/10.1016/j.tecto.2015.07.021
0040-1951/

Lerche, 1991). The rheological coupling at the basin or crustal scale influences the salt mechanics, as observed in places where tectonics is coeval with salt diapirism, such as the Makran accretionary wedge or the Dead Sea (e.g., Graham et al., 2012; Smit et al., 2003, 2008). This is in contrast with areas where salt kinematics was influenced by significant stresses, but basin deformation is minor, frequently occurring in the foreland or hinterland of convergent plate margins. The factors influencing salt mechanics in these situations are less understood and usually inferred as a combination between overburden and far-field transmission of contractional deformation at large distances from the active deformation zone (McClay et al., 2004; Roure, 2008).

The Transylvanian Basin is one such salt-bearing basin formed in the back-arc of the highly bended Carpathians Mountains during the Miocene rollback of a slab attached to the European continent (Fig. 1, e.g., Ciulavu et al., 2000; Ciupagea et al., 1970; Schmid et al., 2008). The basin has a roughly circular geometry and contains up to 4 km thick Middle–Upper Miocene sediments (Fig. 1). The basin evolution was controlled by the coupling between subsidence in its centre and uplift along the South and East Carpathian margins driven by Miocene orogenic events (Matenco et al., 2010). Outside a few low-offset Middle Miocene normal faults (Krézsek et al., 2010), the overall basin geometry is rather simple, gently deepening towards the basin centre, without

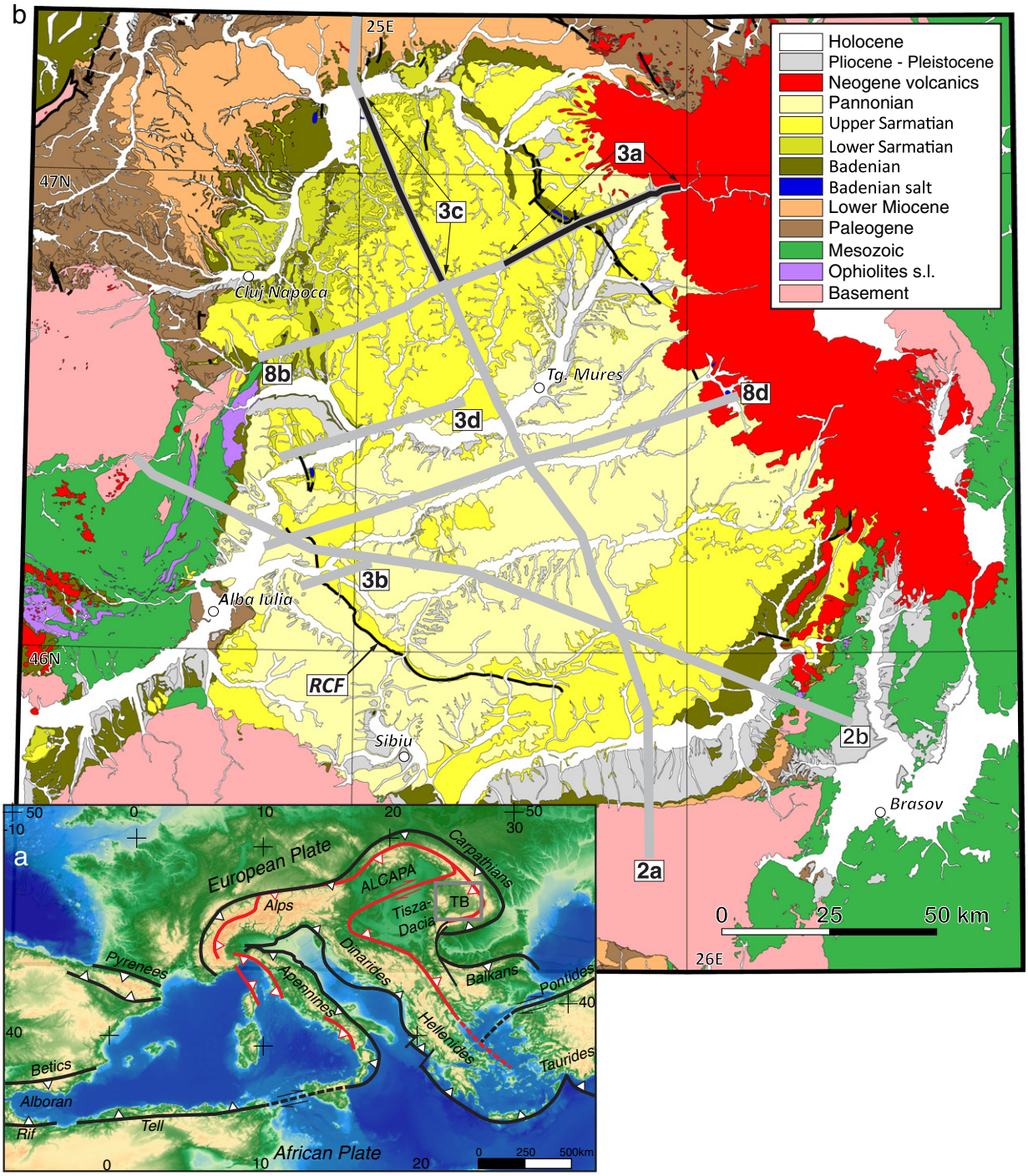

Fig. 1. a) The location of the Transylvanian Basin within the Mediterranean systems (simplified from Ustaszewski et al., 2008; Schmid et al., 2008). b) Simplified geological map of Transylvanian Basin and surrounding orogens (modified from Tilita et al., 2013) with the location of interpreted cross-sections and seismic lines. TB, Transylvanian Basin; RCF, Rusi–Cenade Fault.

any major fault(s) able to explain the observed subsidence (Fig. 2). Given this geometry, the mechanism driving the subsidence and subsequent uplift at the end of Miocene times is still a matter of debate (see Tilita et al., 2013, for a detailed discussion). Deriving the mechanisms responsible for Transylvanian Basin formation and evolution is hampered by widespread salt diapirism that prevents accurate subsidence determinations. Previous 1D or 2D subsidence modelling studies underlined a regional pattern in two stages, tectonic-like subsidence occurring rapidly during Early–early Middle Miocene, followed by reduced late Middle–Late Miocene "sag" subsidence (Ciulavu, 1999; Cranganu and Deming, 1996). However, these studies were inconclusive in deriving the basin evolution, in particular due to salt re-distribution during the successive phases of subsidence and tectonic uplift affecting the basin margins (Matenco et al., 2010). Therefore, a combined subsidence modelling methodology that accounts for 3D salt re-distribution is required to quantify the subsidence and in particular its distribution in the roughly circular geometry of the basin.

We assess the 3D subsidence evolution and salt re-distribution under differential loading in the Middle–Late Miocene Transylvanian Basin. Our study takes advantage of an existing 3D depth geometry derived from the depth-converted interpretation of a large number of seismic lines and subsequently corrected for stratigraphic volumes (Tilita et al., 2013). This geometry is composed of depth and thickness maps for all Miocene stratigraphic intervals that cover the entire extent of the basin and was used as an input to numerical modelling. A dual backward and forward numerical modelling salt re-distribution approach was used, which has been previously applied in the study of salt movements elsewhere (Maystrenko et al., 2013; Scheck and Bayer, 1999; Scheck et al., 2003). The backward modelling approach reconstructs the evolution of salt influenced by all factors, including overburden and erosional removal, tectonic vertical movements and intraplate stresses. The forward modelling reconstructs the evolution of salt, as it would have been driven only by the evolution of overburden/erosional removal influenced by tectonic subsidence. The differences between the evolutionary stages obtained in the two numerical approaches are likely the expression of intraplate stresses. The results of the salt redistribution modelling were constrained with syn-kinematic depositional patterns observed by basin seismostratigraphic interpretations. The modelling of tectonic subsidence and uplift inferences were correlated with other existing basin studies and kinematic/exhumational studies in the orogens surrounding the basin. This allows us to quantify the 3D evolution of subsidence and salt migration with time, quantify the role of intraplate stresses during the Miocene evolution of the Transylvanian Basin and, possibly, provide new critical inferences for the cause(s) of the Middle Miocene basin subsidence.

2. Evolution of the Transylvanian Basin and neighbouring areas

The Miocene evolution of the SE segment of the Carpathian Orogen and its hinterland basins (Fig. 1a) was driven by the subduction rollback of a slab thought to be derived from the Alpine Tethys (e.g., Schmid et al., 2008). This slab was attached to the cratonic units of the East European, Scythian and Moesian foreland during Cretaceous to Miocene episodes of subduction and collision (Merten et al., 2010; Săndulescu and Visarion, 1988; Visarion et al., 1988). At the interior of the Carpathians, the Miocene sediments of the Pannonian and Transylvanian basins overlie a Cretaceous–Paleogene orogenic area composed by nappe stacks grouped in two mega-units (i.e., ALCAPA and Tisza-Dacia, Fig. 1a, Csontos and Vörös, 2004).

The Transylvanian Basin (Fig. 1b) overlies the basement and sedimentary cover of the Tisza and Dacia units and their suture zone (Csontos and Vörös, 2004; Săndulescu and Visarion, 1977; Schmid et al., 2008). These units consist of thick-skinned nappes emplaced during the Cretaceous closure of the Ceahlău-Severin and Neotethys oceans (e.g., Haas and Péró, 2004; Iancu et al., 2005; Kounov and Schmid, 2013; Săndulescu, 1988; Schmid et al., 2008). Their late Jurassic–late Early Cretaceous suture zone (i.e., the Transylvanides nappes, Săndulescu and Visarion, 1977) is made up of Jurassic ophiolites, island-arc volcanics and their sedimentary cover (Figs. 1 and 2, Hoeck et al., 2009; Ionescu et al., 2009; Nicolae and Saccani, 2003; Robertson et al., 2009; Schmid et al., 2008). These units and

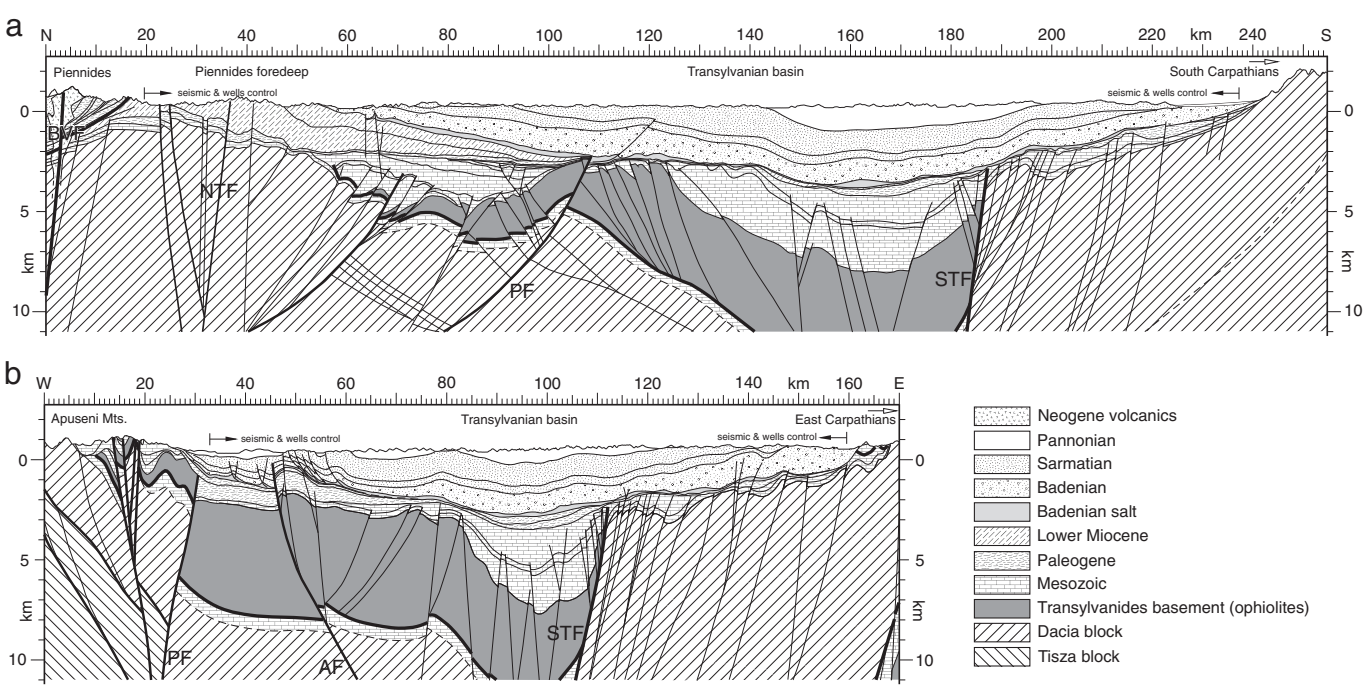

Fig. 2. Regional geological cross sections over the Transylvanian Basin derived from seismic interpretation studies (modified from Tilita et al., 2013). a) N–S cross-section over the Transylvanian Basin linking the Piennides thrust system with the South Carpathians. b) WNW–ESE cross-section in the southern part of the Transylvanian Basin from the Apuseni Mountains to East Carpathians. Locations of the cross sections are shown in Fig. 1. NTF, North Transylvanian Fault; STF, South Transylvanian Fault; PF, Puini Fault; AF, Appulum Fault.

their suture zone were affected by successive deformation events that include Late Cretaceous shortening and subsequent extension, followed by two other latest Cretaceous–Paleocene and Late Eocene–Oligocene periods of contractional deformation (Fig. 2, e.g., Balintoni, 1996; Haas and Péró, 2004; Kounov and Schmid, 2013; Krézsek and Bally, 2006; De Broucker et al., 1998; Merten et al., 2011). The latter tectonic episodes created significant uplift associated with general erosion in most of the basin (e.g., Paraschiv, 1997; Tilita et al., 2013). The exception is the northern part of the Transylvanian Basin, where thrusting of the ALCAPA over Tisza-Dacia mega-units created a Late Oligocene–Early Miocene foredeep, which was subsequently tilted by Miocene vertical movements (northern parts of Figs. 2a and 3c, Csontos and Nagymarosy, 1998; Tischler et al., 2007, 2008).

2.1. The post-Early Miocene evolution of the Transylvanian Basin

The Carpathian subduction and collision closed a large gulf of oceanic to thinned continental crust that existed at around 20 Ma in the European domain (the Carpathians embayment, e.g., Ustaszewski et al., 2008). This resulted in the 160–200 km of shortening recorded by the thin-skinned nappes of the East Carpathians (e.g., Morley, 1996; Roure et al., 1993) and transcurrent to contractional deformation observed the South Carpathians and their foreland (Krézsek et al., 2013; Răbăgia et al., 2011). This was followed during the Pliocene–Quaternary by out-of-sequence thrusting related to the late evolution of the presently observed Vrancea slab in the SE Carpathians corner (Cloetingh et al., 2004, 2005; Ismail-Zadeh et al., 2012; Martin et al., 2006; Matenco

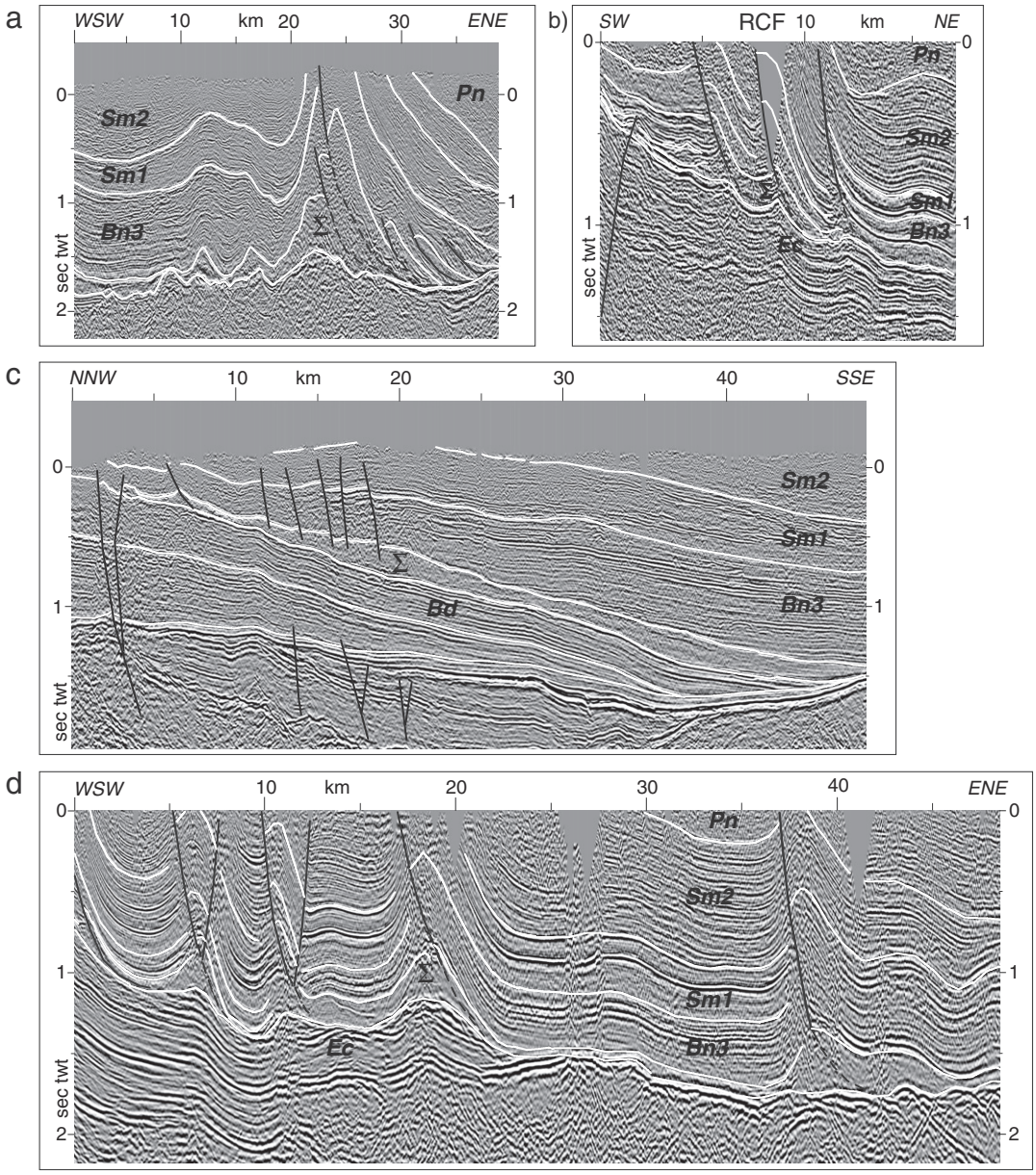

Fig. 3. Interpreted seismic lines illustrating the kinematics of salt in the Transylvanian Basin. Note that the resolution of seismic lines prevents the interpretation and correlation of stratigraphic sequences with reduced thicknesses, such as the Lower Badenian or locally Oligocene. Ec, Eocene; Bd, Burdigalian; Σ, Middle Badenian salt; Bn3, Upper Badenian; Sm1, Lower Sarmatian (i.e. Lower Volhinian); Sm2, Upper Sarmatian (i.e. Upper Volhinian–Bessarabian); Pn, Pannonian. Location of seismic lines is displayed in Fig. 1. a) Interpreted seismic line crossing the large-scale salt diapir located in the NE part of the basin, in the vicinity of the overlying volcanic sequence. b) Interpreted seismic line in the SW part of the basin crossing the Rusi–Cenade fault system. Note the coupled thrust-salt décollements that transfer rapidly offsets along their strike. c) Interpreted seismic line in the northern part of the basin where the apparently less deformed salt layer overlies the tilted Lower Miocene foredeep wedge of the Piennides. d) Interpreted seismic line in the central–western part of the basin, where apparently symmetric salt pillows are in fact associated with thrust offsets that demonstrate top-W direction of transport.

et al., 2007; Oncescu and Bonjer, 1997; van der Hoeven et al., 2005). This Miocene–Quaternary shortening has resulted in a number of Middle Miocene uplift events affecting the East and South Carpathian margins of the Transylvanian Basin that cumulatively reach 5–6 km (Matenco et al., 2010; Merten et al., 2010). In the back-arc domain, the slab rollback is responsible for the Miocene extensional opening of the Pannonian Basin (e.g., Horváth et al., 2006). This extension decreases eastwards and has negligible effect in the eastern part of the Apuseni Mountains and Transylvanian Basin (Fig. 3, e.g., Krézsek et al., 2010; Tilita et al., 2013). The subduction and genetically related extensional back-arc evolution also caused the widespread Miocene–Pleistocene volcanism of the intra-Carpathian area (Mason et al., 1998; Pecskay et al., 1995; Seghedi et al., 2004; Szabo et al., 1992), large volumes of volcanics and volcanoclastics being emplaced in particular along the eastern margin of the Transylvanian Basin (Fig. 1). The overall uplift of the SE European mountain chains separated the Paratethys endemic domain from the main Tethyan realm starting with the Oligocene (Senes, 1973; Steininger et al., 1988), while the Carpathians separated the Central Paratethys area of the Pannonian and Transylvanian basins starting with Late Miocene times, creating an endemic domain characterised by a separate biostratigraphy (Fig. 4, Magyar et al., 1999; Rögl, 1999).

In the Transylvanian Basin, a regional marine transgression took place during early Middle Miocene times (Early Badenian) and led to the deposition of 100–200 m thick siliciclastic sediments (e.g., Filipescu and Gîrbacea, 1997). These deposits are likely the result of syn-kinematic sedimentation associated with small-offset normal faults (Krézsek et al., 2010). The onset of regional volcanism led to the deposition of the ~50 m thick Dej Tuff complex (Fig. 4, 14.37–14.38 Ma, de Leeuw et al., 2013; Seghedi and Szakacs, 1991). The Badenian salinity crisis recorded at the scale of the entire Carpathians was probably associated with a regional sea-level fall (de Leeuw et al., 2010; Peryt, 2006) and resulted in evaporitic deposition in the central and eastern parts of the Transylvanian Basin in either a lagoonal (Paucă, 1968) or a deeper water environment (Krézsek and Bally, 2006). Near the basin margins, gypsum was deposited in a sabkha-type environment (Ghergari et al., 1991). In fact, the deposition of the evaporitic sequence took place likely in a deeper, but desiccated marine environment, reaching thicknesses in the order of 300 m (Krézsek and Bally, 2006).

Large scale Miocene subsidence is recorded in the Transylvanian Basin during Late Badenian times and is reflected by a transgressive phase followed by a high-stand system tract (Krézsek and Filipescu, 2005; Matenco et al., 2010), overlain by a thin volcanoclastic sequence (the Borşa–Apahida–Iclod–Turda tuffs, Fig. 4). Depositional environments

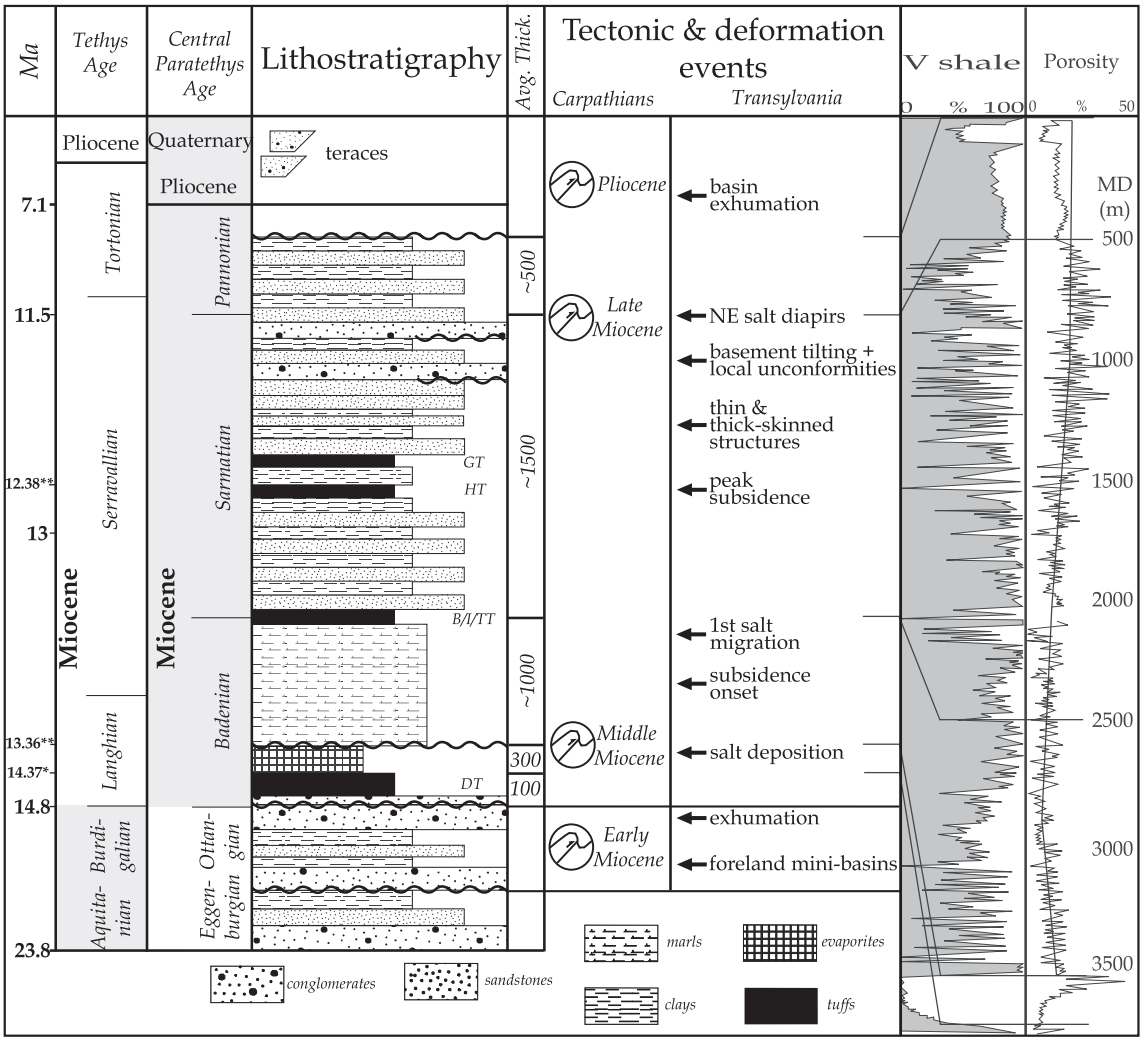

Fig. 4. Simplified tectono-litho-stratigraphic column of the Transylvanian Basin (compiled from Ciulavu et al., 2000; Ciupagea et al., 1970; De Broucker et al., 1998; Krézsek and Filipescu, 2005). The right part of the column is interpreted shale volume (*Vshale*) curve and porosity curve for a representative well located in the centre of the basin, which drilled the entire Middle–Upper Miocene sequence. Note that the vertical scale of the two columns is different, i.e. stratigraphic thickness versus well measured depth. *After Seghedi and Szakacs (1991). **After de Leeuw et al. (2013). DT, Dej tuff; B/I/TT, Borşa–Apahida, Iclod, Turda tuffs; HT, Hădăreni tuff; GT, Ghiriş tuff.

were mostly deep marine (marls and black shales), with local shallow water shelf and slope. During Sarmatian times, sedimentary environments shifted from marine to brackish and lacustrine during the gradual closure of the Central Paratethys and were influenced by a significant number of relative sea-level variations (Krézsek and Filipescu, 2005). These sediments are made up of fine to coarse-grained clastics, evaporites and numerous levels of interbedded volcanoclastics. The depositional environment was slope to deep marine composed of submarine fans and distal pelagic, condensed layers, incised valleys, deltas and fan deltas (Krézsek and Filipescu, 2005). Frequent sea-level variations formed surfaces that recorded minor amounts of erosion in the S and SE marginal parts of the basin. Another regional transgressive event is recorded at the beginning of Pannonian times (Filipescu and Gîrbacea, 1997; Sztanó et al., 2005), possibly in response to the complete endemic closure of the Central Paratethys (ter Borgh et al., 2013). The Transylvanian Basin became a lacustrine environment, where frequent base-level variations created a mix of shallow environments with interbedded lacustrine fans, low-stand deltas and sandy deltas, while coarse-grained sediments accumulated in eastern proximal areas. The central and western distal parts received mainly pelagic sediments with frequent influxes of low-energy turbidites (Krézsek et al., 2010; Sztanó et al., 2005). The entire Transylvanian Basin was uplifted close to its present day elevations of 250–600 m towards the end of Pannonian times, the erosion resulting in the deposition of continental alluvial and locally reduced lacustrine sediments (Matenco et al., 2010). The thick sediment loading coupled with nearby orogenic uplift, deposition of large volumes of overlying volcanics and the intraplate compression were interpreted to be responsible for the observed widespread salt diapirism in the Transylvanian Basin (Krézsek and Bally, 2006; Szakacs and Krézsek, 2006; Tilita et al., 2013). However, little is known on kinematic evolution of this diapirism and quantification of its driving mechanisms.

3. Salt kinematics in the Transylvanian Basin

The geometry of the salt structures in the Transylvanian Basin has been described with various degrees of details by a large number of studies (e.g., Krézsek and Bally, 2006; Mrazec, 1932; Tilita et al., 2013, and references therein). For the purpose of this study we will describe only the main features relevant for the numerical modelling of salt re-distribution. Various forms of salt structures are present all-over the basin (Figs. 2 and 3). Two main salt lineaments are observed, one along the eastern basin margin and one in the central-western part of the basin (Figs. 1 and 5). Diapirism created salt domes that locally are close to or reached the surface, salt pillows associated with open folding in the overlying sequence, décollement related thrusts in the salt and gravitational collapse structures due to lateral salt migration (Figs. 1 and 3, see also Tilita et al., 2013). The migration of salt was associated with the formation of rim synclines with onlapping geometries, changes in strata thickness and erosion of sediments uplifted by diapiric movements (Fig. 3). These syn-kinematic sediments suggest continuous salt

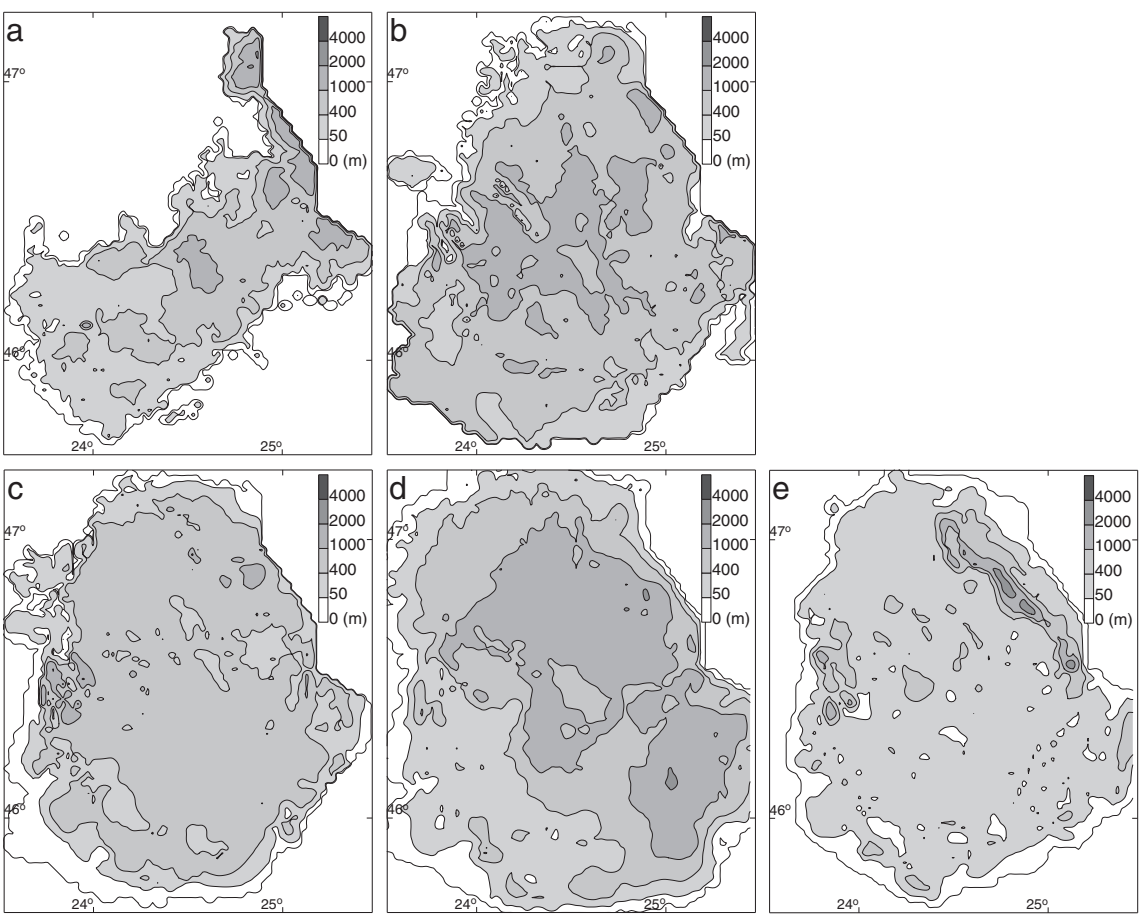

Fig. 5. Vertical thickness maps of the stratigraphic horizons in the Transylvanian Basin that were used as input for the 3D subsidence and salt re-distribution modelling in the 3D crustal model. The original maps published by Tilita et al. (2013) were corrected for intersections in order to build spatially consistent voxels with a horizontal resolution of 2 km by using the Geological Modelling System (GMS, Scheck et al., 2003). In few situations, the various units pinch-out laterally and their continuation was interpreted according to their geological meaning (such as unconformities, non-deposition or lateral termination of sedimentation). The overall effect of these local unconformities in the volume restoration of sediments in the basin is rather minor. a) Thickness map of the Pannonian strata. b) Thickness map of the Upper Sarmatian strata. c) Thickness map of the Lower Sarmatian strata. d) Thickness map of the Upper Badenian strata. e) Thickness map of the Middle Badenian salt sequence. In order to account for the effects of the Pliocene–Quaternary erosion, the 3D geometrical model has been truncated to the same horizontal reference level, i.e. assuming complete basin fill at the end of Pannonian times.

migration since the Late Badenian, with two peak phases during Late Sarmatian and Late Pannonian times (Fig. 3a, b and d). After basin exhumation at the end of the Miocene, the salt continued its migration, as demonstrated by truncation of Upper Pannonian strata (Fig. 3a). In most situations, the offset analysis combined with syn-kinematic depositional patterns indicated most of the shallow thrusts rooted in the salt layer post-date the Sarmatian (e.g., Fig. 3a, b and d). Most of these faults offsets are Pannonian or younger in age.

In more details, the centre of the basin displays symmetrical diapiric structures organised in low-amplitude pillows, the salt thicknesses being in the order of tens to hundreds of metres (Fig. 2). Near the NE border of the basin a massive, up to 2.5 km thick salt dome is observed tilting the overlying sediments, partly piercing them and locally reaching the surface (Figs. 1b and 3a). The internal geometry of the uplifted area and its flanking sediments suggests that salt has migrated from two directions into the diapir (Fig. 3a). The movement from the NE margin into the diapir is demonstrated by syn-kinematic deposition and numerous shallow décollement related thrusts with WSW-ward vergence that often transfer offset along their strike. This geometry and timing of deformation is in agreement with the idea that the volcanic sequence emplaced over the entire sedimentary sequence at the end of Miocene times (Fig. 1b) induced sagging, the W-wards movement of the salt away from the volcanic loading being facilitated by the locally high geothermal gradient (Szakacs and Krézsek, 2006). Along the western flank of this diapir, the geometry of syn-kinematic deposition, combined with sagging structures such as turtle anticlines, demonstrate an opposite ENE-ward sense of movement of the salt into the diapir (Fig. 3a). Therefore, the geometry of this particularly large structure suggests a two-way migration of salt into the diapir.

A number of shallow thrusts associated with salt diapirs grouped under the generic name of the Rusi–Cenade Fault are observed near the SW margin of the basin (Fig. 1b, Ciulavu et al., 2000). This zone of deformation is made up by a laterally changing number of near surface, W to SSW vergent salt-décollements, which transfer their offsets along the strike (Fig. 3b). In fact, the strike of this fault system follows the curved geometry of the South Carpathians–Apuseni Mountains basin border (Fig. 1). This geometry combined with the configuration of syn-kinematic sediments indicates that salt has migrated from the centre of the basin towards its western and southern margin during late Sarmatian–Pannonian times (Fig. 3b). North of the only significant basin thrust that crosscuts the salt layer (the Appulum Fault, Fig. 2b), the central-western margin of the basin is made up by a number of apparently symmetrical salt pillow structures (Fig. 5e). These pillows are associated with shallow décollements that show a dominant W-ward vergence, associated with the same type of second-order opposite vergent structures along local pop-ups (Fig. 3d). This geometry combined with Late Badenian–Pannonian syn-kinematic sedimentation suggests a gradual W-wards salt migration at lower rates than the ones observed S-wards.

The basement of the basin gradually deepens S-wards, an effect of the Miocene subsidence that tilted the earlier deposited Upper Oligocene–Lower Miocene foredeep (Fig. 3c). Small-scale pillows and collapse structures associated with Late Badenian–Late Sarmatian syn-kinematic sediments suggest reduced N-ward salt migration.

All these characteristics demonstrate an overall migration of salt towards the basin margins at variable rates during the Late Badenian–post-Pannonian times, with the notable exception of the NE located salt wall, where a short range opposite migration towards the centre of the basin was driven by volcanic sagging.

4. Backward and forward subsidence modelling of salt kinematics

Subsidence analysis techniques applied to basins affected by significant salt diapirism are commonly performed as 2D restorations of depth converted seismic sections (e.g. Rowan, 1993; Rowan and Ratliff, 2012; Schäfer et al., 1998; Stewart et al., 1996; Zirngast, 1996). Such techniques take into account decompaction of unloaded sediments, restoration of fault displacements, or isostatic rebound (e.g. Buchanan et al., 1996; Schäfer et al., 1998). Other techniques combine backstripping with salt restoration assuming different rheologies for the salt and its overburden layers (Ismail-Zadeh et al., 2001). Movements perpendicular to the plane of cross section that cannot be quantified affect significantly 2D restorations of salt movements. Existing 3D restorations of salt movements assume a relationship between down-building and salt withdrawal, relating the thickness of peripheral sinks to the amount of salt withdrawn from the corresponding area (Zirngast, 1996). Alternatively, other studies assume a balance between the amounts of salt migration and sediments deposited when the effects of isostatic loading, sedimentary compaction and erosion are removed (Schäfer et al., 1998; Whitefield et al., 1999; Yin and Groshong, 1999). In our study, we apply a more straightforward technique in which the motion of salt is restored for each backstripping step (Scheck et al., 2003). This method allows redistributing the salt in 3D in response to the actual overburden load, while conserving the volume.

4.1. Modelling principles

We apply a salt forward and backward subsidence restoration technique described in Scheck and Bayer (1999) and Scheck et al. (2003). This model assumes that salt behaves as a viscous fluid, which is consistent with tectonic and kinematic observations (e.g. Davison et al., 1995; Schultz-Ela et al., 1993; Vendeville and Jackson, 1992), analogue (e.g. Koyi et al., 1993; Nalpas and Brun, 1993; Vendeville et al., 1995) and numerical modelling (Podlachikov et al., 1993; Poliakov et al., 1993; van Keken et al., 1993). Furthermore, the response of the salt to changes in overburden load is considered as resulting in a hydrostatic equilibrium between the salt and the overburden. This means that the salt top deformation is changing dependent on the load exerted by the overburden.

The assumption of hydrostatic equilibrium in the salt and the fluid-like behaviour of the salt are also in agreement with the observation that salt provides an efficient rheological decoupling layer in the Transylvanian Basin. The structural style in the underlying basement is significantly different than in the overlying cover. Very few faults crosscut the salt layer, the deformation of the Miocene cover being almost entirely restricted to shallow décollement and folds rooted in the salt itself.

The volume of salt in the subsurface of the basin is considered constant with time, as the salt is assumed to be an incompressible fluid that was not affected by significant surface erosion or solution processes. This is in agreement with observations that salt crops out in the Transylvanian Basin with small areal extent, indicating that erosion was minor when compared with the actual bulk volume of the salt. The model also assumes that the base of the salt (and its "basement") is the reference surface where the pressure is equilibrated. In other words this means that the cumulative loads of overburden sediment and the salt are equal at the salt basement surface for the same depth.

The input for the model is the 3D structural and litho-stratigraphical geometry of the Transylvanian Basin. This geometry has been constructed by interpreting of a large number of industrial seismic lines calibrated with wells (see Tilita et al., 2013) and is in agrement with other seismic interpretations in the basin, wherever available (De Broucker et al., 1998; Krézsek and Bally, 2006; Krézsek and Filipescu, 2005; Krézsek et al., 2010). The structural model resolves the 3D present-day geometry of five different layers in the salt overburden, including the ones of the Pannonian, Upper and Lower Sarmatian, the Upper Badenian deposits and the Middle Badenian salt layer (Fig. 5). The geometry of the various layers has been corrected for intersections in order to build a spatially consistent 3D structural model with a spatial resolution of the composing 2D thickness grids of 2 km by using the Geological Modelling System (GMS, developed by GeoForschungsZentrum Potsdam). The loss of stratigraphy by salt piercing through the overburden was estimated by

gradually adding or subtracting stratigraphy over the pierced area to the level of the present day topography. The thicknesses of stratigraphic layers are extrapolated from neighbouring areas that are not affected by salt movement in the centre of the diapir or in the peripheral sinks (for a similar procedure, see also Scheck et al., 2003).

The model assumes that every layer is characterised by uniform lithologies and therefore constant physical properties have been assigned to each layer, including load-porosity-dependent densities and associated compaction factors, derived from wireline logging data from several wells (Fig. 4). In general, the siliciclastic sediments of the Transylvanian Basin have average porosities ranging from 20–25% near surface to 10–20% at greater depths (Fig. 4). Therefore, the compaction in the basin is significant and has been included in the calculations of tectonic subsidence.

Detailed geometry of every constitutive layer, along with their average lithology enabled the calculation of the 3D sedimentary load using a finite element method (Scheck et al., 2003). Based on this 3D load distribution a crustal model was calculated assuming Airy isostasy. The isostatic calculation takes into account the overall geometry and composition of the pre-Neogene strata and the underlying crustal thickness derived from available deep geophysical studies (Diehl et al., 1983; Rădulescu, 1988). This initial model of the present-day structural and density configuration provided the starting point for the backstripping and salt restoration procedure. Accordingly, a further assumption is that the density distribution in the crust is at any given time in isostatic equilibrium with a given Moho position (e.g., Maystrenko et al., 2013; Scheck and Bayer, 1999; Scheck et al, 2003).

4.2. Modelling technique

Two models were constructed and tested. Both techniques (backward and forward) handle the sedimentary load including compaction/decompaction, salt re-distribution to equilibrate overburden and isostatic compensation at each step. The backward model reconstructs the subsidence in 3D, obtained by successive steps of backstripping by calculating at each step the individual salt-redistribution driven by the change in overburden due to gradual removal of layers. The calculation continued until the base of the salt reached a hydrostatic equilibrium. In other words, the salt was allowed to flow to reach this equilibrium. Therefore, the redistribution affected the salt and its overlying sedimentary layers, whereas the basement below remained unchanged. More specifically, at each step the modelling required the removal of a cover layer, redistribution of the salt until the load above salt is equilibrated, decompaction of remaining layers, followed ultimately by calculating the isostatic response of the mantle to total reduction in crustal load after stripping of the layer and salt redistribution. The latter means that the hydrostatically balanced geometry of the salt and overburden is in local isostatic compensation with the entire model. This procedure of backstripping, salt redistribution and isostatic compensation has been applied to five successive steps backwards in time from the end of the Pannonian times to the end of salt deposition at the end of the Middle Badenian. For further details on the backward approach we refer to Scheck et al. (2003).

The forward modelling starts with a restored initial salt geometry in isostatic equilibrium that is successively loaded by the corrected thickness of overlying layers in the same 5 successive steps until the end of Pannonian times. In more detail, the procedure involved a sequence of removal of all layers including the salt, decompaction and isostatic equilibration of the crustal response to obtain a pre-salt paleo-topography. This surface was loaded with the salt layer that was then re-distributed by the renewed isostatic compensation. This was followed by deposition of first overburden layer, redistribution of the salt in response to the new load conditions above the salt and renewed isostatic compensation. This procedure was repeated for the deposition of each successive salt cover layer (see Ismail-Zadeh et al., 2004; Maystrenko et al., 2006; van Wees and Beekman, 2000, for further details).

What is the difference between the two types of models and why do we need them both? The backward modelling reconstructs directly the basin evolution, influenced by all external and internal factors acting in the basin, including overburden and erosional removal, tectonic vertical movements and intraplate stresses. The forward modelling reconstructs a possible basin evolution, as it would have been driven only by salt re-distribution beneath the overburden/erosional removal, including the tectonic subsidence. The differences between the evolutionary stages obtained in the two numerical approaches are the expression of intra-plate stresses and the misfit generated by the (lack of) precision of our assumptions.

The largest uncertainty in our modelling approach is related to estimates of erosion. The basin lacks regional unconformities, while local unconformities formed near the basin margins during moments of Carpathians exhumation are rather negligible at the scale of the basin, such as the Lower Sarmatian unconformity near the SE margin of the basin (south of km 220 in Fig. 2a). The most significant is the erosion post-dating the basin uplift at the end of Miocene time. Our assumption that the sedimentation extended to the maximum present-day elevation of the basin of ~600 m is in agreement with thermochronological studies in the neighbouring orogens (see discussion in Matenco et al., 2010). However, this assumption has a larger error bar and is significant in calculations. We note therefore that the first stage of the backward modelling procedure and the last stage of the forward modelling include both the deposition of the Pannonian strata and the subsequent erosion. The possible error of our erosional assumption is, therefore, included in the difference between the results of the backward and forward modelling, i.e. influencing our inferences on intraplate stresses. Similar uncertainties are related to the above-mentioned procedure of estimating the loss of stratigraphy by erosion in salt piercing by gradually adding or subtracting stratigraphy from neighbouring areas. These errors become evident during salt-redistribution modelling by artefacts either in undeformed state or by comparison between the two modelling approaches and are discussed below. Such errors are fairly local over the salt diapirs and do not influence the regional inferences our modelling.

Other uncertainties may be related to the geometry of our seismic and well data that controls our structural model. Although the coverage with seismic lines and wells is relatively high for a modelling study (see Tilita et al., 2013), much less such data are available in the shallow parts of the basin near its margins. Although supplemented by surface information derived from geological maps and personal field observations, the error bar of the structural model in these marginal areas remains in the order of up to 200 m. Given the limited extent of these areas, the impact of potential errors in our inferences is rather reduced. Other uncertainties are related to the lack of precision of interpreting highly inclined strata on the flanks of salt diapirs, depth conversions employing average interval velocities at the scale of the entire basin, or averaging porosities, densities and lithologies per intervals in the subsidence analysis. All these uncertainties are common in any subsidence analysis. In our study we estimate that these are in the order of tens of metres and, therefore, negligible at the scale of our analysis.

5. Subsidence and salt re-distribution modelling results

The analysis of Miocene tectonic subsidence coupled with the Middle Miocene salt migration suggests that the evolution of salt was more dynamic than just a simple migration towards the basin margins.

5.1. Back-ward modelling of salt kinematics and tectonic subsidence

The restored geometry of the salt layer at the end of its deposition indicates an average depositional thickness in order of 500 m, but with a variable geometry organised in a central depocentre and a local

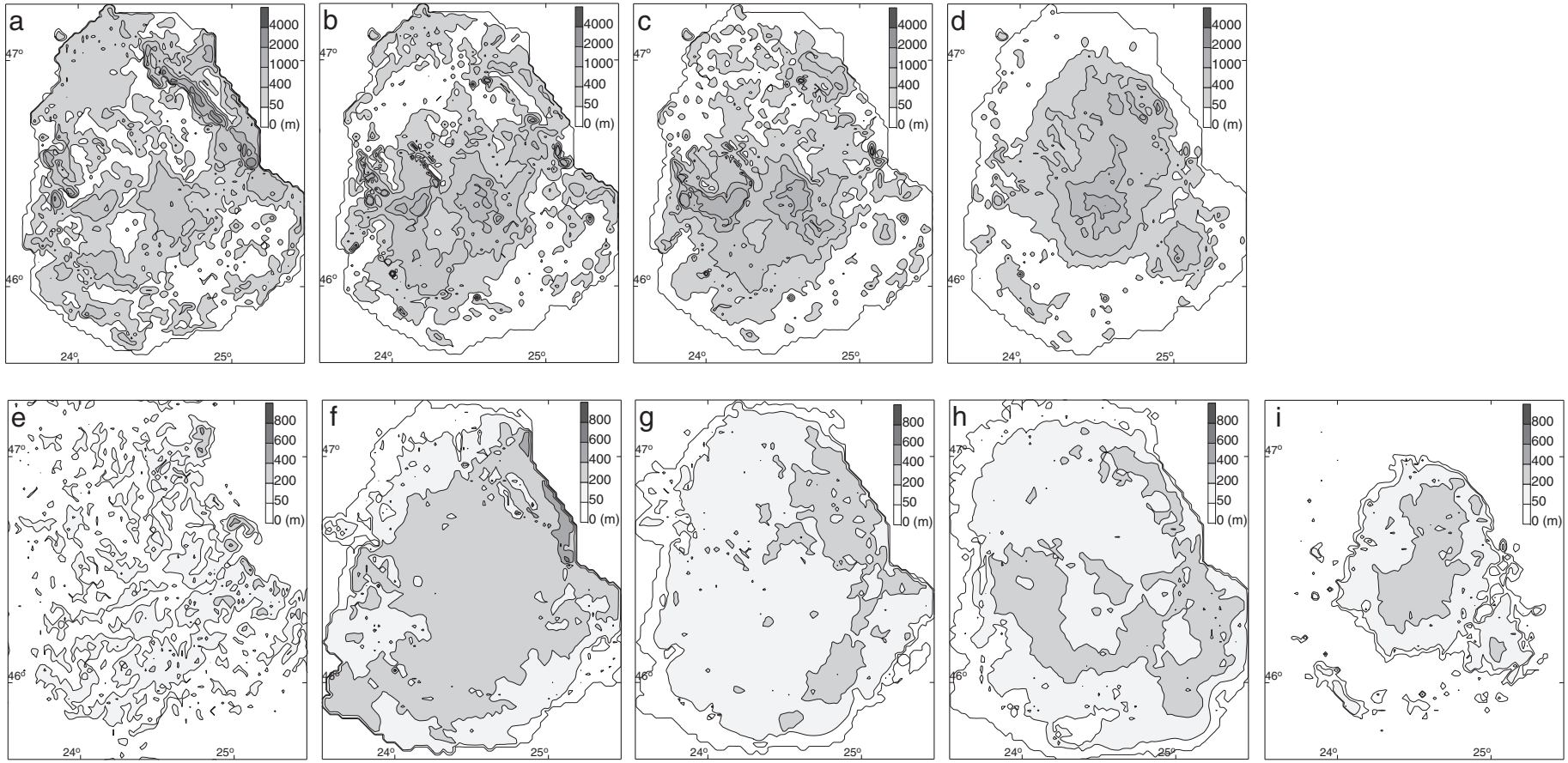

Fig. 6. Results of the computed models for salt re-distribution in the basin and tectonic subsidence derived by backward modelling. a) Modelled salt geometry at the end of Upper Sarmatian times. b) Modelled salt geometry at the end of Lower Sarmatian times. c) Modelled salt geometry at the end of Upper Badenian times. d) Modelled salt geometry at the end of Middle Badenian salt deposition. e) Modelled tectonic subsidence for Pannonian times. f) Modelled tectonic subsidence for Upper Sarmatian times. g) Modelled tectonic subsidence for Lower Sarmatian times. h) Modelled tectonic subsidence for Upper Badenian times. i) Modelled tectonic subsidence for Middle Badenian times.

one located in the SE (Fig. 6d), where the reconstructed salt thickness reached more than 1 km.

At the end of the Badenian times (Fig. 6c) a significant volume of salt had already migrated from the main depocentre towards W and SW parts of the basin, while the small SE depocentre dissipate, the salt probably migrated towards central areas. The model suggests that an increased salt concentration near the NE basin border was already present at the end of Badenian times by migration from the basin centre, in agreement with inferences from syn-kinematic sediments observed along the western flank of the salt wall (Fig. 3a).

Elsewhere, a smaller-scale migration of salt towards the basin margin is observed N- and S-wards and, surprisingly, from the basin SE margin towards its centre (Fig. 6c). Indeed, the latter migration of salt is constrained by the observed presence of syn-kinematic Upper Badenian sediments, but its direction of migration is not obvious in the interpretation of seismic lines (Tilita et al., 2013). These patterns are the result of the asymmetric deposition of Badenian sediments that are thick in the SE areas and decrease towards the basin centre (right part of the cross-section in Fig. 2b).

These migration patterns continued during Early Sarmatian times. Towards the end of this period (Fig. 6b), the two main areas of maximum thicknesses are still preserved in the centre-east and centre-west, although a larger quantity of salt from these domains has migrated elsewhere. Near the NE margin of the basin a rather continuous layer of salt is observed that gradually started to be connected with local accumulations more to the SE. The formation of pillow diapirs is observed along the western part of the basin, in agreement with the syn-kinematic patterns of deposition of Lower Sarmatian sediments observed in seismic lines (Fig. 3d).

Late Sarmatian is a period of major re-organization of salt in the basin (Fig. 6a), its migration creating geometries that resemble its present-day distribution (Fig. 5e). The asymmetric deposition of Upper Sarmatian strata induced lateral migration of salt from domains affected by the load of these depocentres towards the basin margins (Fig. 6a). This response of the salt to the larger thickness of Upper Sarmatian deposits in the basin centre (Fig. 5b) caused a significant change of the salt configuration compared to the previous Lower Sarmatian salt distribution. The maximum salt thickness reconstructed for Late Sarmatian times in the centre of the basin is still preserved in a relatively larger area. Near the basin margins, the migration of the salt is observed by the initiation of salt accumulation in the Rusi–Cenade system. The model also suggests that large amounts of salt had already moved into the large salt dome located in the NE (Fig. 6a).

After the Sarmatian, the deposition of thick Pannonian strata in the centre of the basin (Fig. 5a) has caused large-scale salt migration leading to a decrease of the former maximum accumulation in the centre of the basin by migration and enhancing the diapiric growth towards its margins where most of the associated shallow décollements formed or increased their offsets. The migration should have decreased once the basin was uplifted and sediments removed by erosion starting at the end of Miocene times.

According to the models, tectonic subsidence shows different patterns across the basin during the Middle–Late Miocene (Fig. 6e–i). Large amounts of tectonic subsidence took place already during the Middle Badenian salt deposition in the central basin depocentre, slightly expanding towards the SE (Fig. 6i). This subsidence coeval with salt deposition has not been detected by previous tectonic reconstructions, but is rather logical in order to justify the accumulation of more than 1 km of salt in the centre of the basin, where subsidence should have kept pace with desiccation and deposition (Fig. 6d).

The model further predicts important amounts of tectonic subsidence near the East and SE Carpathians margin during Late Badenian times (Fig. 6h). This new inference is in agreement with the asymmetric sedimentation in respect to the present geometry of the basin and thick coeval sedimentation in these parts of the basin (Fig. 5d). Note that at higher resolution the large amounts of subsidence inferred in the area of the NE salt wall (Fig. 6h) may be an artefact of under-estimating the eroded Upper Badenian strata, as the subsidence was possibly more distributed in this region.

Interestingly, the model predicts large amounts of Late Badenian tectonic subsidence in a depocentre located in the western parts of the basin, where the coeval sedimentation is rather reduced. This is the result of salt migration during Late Badenian times in the same area (Fig. 6c). In other words, salt may have filled by migration the space created by tectonic subsidence, resulting in reduced amounts of coeval sedimentation (compare Fig. 6h with c and 5d). In contrast, this migration is also responsible for the reduced amounts of tectonic subsidence recorded the central parts of the basin. Here, the model suggests that the accommodation space for the thick Late Badenian sediments was created by the lateral migration of salt outwards, no significant tectonic subsidence being required.

The Early Sarmatian tectonic subsidence decreased, with the notable exception of two areas located near the East and SE basin margins (Fig. 6g). During the Late Sarmatian, the model still indicates significant tectonic subsidence in the entire basin, with peaks concentrated near the NE margin of the basin (Fig. 6f). Hence, resemblances with the salt diapir geometries in the latter area and in some of the SW parts of the basin may be artefacts due to errors in estimating the eroded Upper Badenian strata, as the subsidence had a possible regional distribution. In contrast to the Late Sarmatian, the Pannonian shows reduced tectonic subsidence (Fig. 6e), the higher values being scattered in small patches distributed everywhere in the basin. Though some short-wavelength variations may indicate late salt movements and associated mini-basin formation, this distribution rather mimics the rough topography of the Transylvanian Basin and is likely derived from errors in estimating erosion. An exception is possibly provided by the NE margin of the basin, where scattered patches of subsidence may isolate a regional pattern of increased tectonic subsidence. Therefore, modelling suggests a major change taking place in the basin from Sarmatian to Pannonian times, changing from enhanced tectonic subsidence to sediments filling a space already created in the basin.

5.2. Forward modelling of salt kinematics and tectonic subsidence

The forward modelling of salt-redistribution and tectonic subsidence during the Middle–Late Miocene has a similar evolution, although the final stage of the model is significantly different from the real present-day geometries. The pre-salt paleo-topography loaded with the isostatically compensated salt layer has resulted in high thicknesses in the centre of the basin (Fig. 7a). When compared with the backward model, no local salt depocentre is predicted in the SE part of the basin (Figs. 6d and 7a). Similar to the backward model, the forward modelling suggests that salt migrates rapidly during Late Badenian times towards one major thickness maximum located in the centre–west and another one NE-wards, although at higher rates and with less amount of salt remaining in the previous basin centre (Fig. 7b). A similar pattern of salt geometry is also predicted for the Lower Sarmatian, although the migration into local salt structures can already be observed (Fig. 7c).

The difference in salt migration trends between forward and backward models becomes evident starting with the Late Sarmatian, the forward model showing other patterns when compared with the backward model and with the present-day geometries (compare Fig. 7c and d, with Figs. 6a, b and 5e, respectively). Although the first order patterns in the organization of diapirs and lateral variations in salt thickness are similar, the forward model suggests that salt should have migrated in large quantities W-wards and SW-wards, whereas only limited NE-ward migration and almost no SE-ward migration is predicted (Fig. 7d, e). In other words, the prediction of the forward model is that most of the salt would migrate W-, SW- and NW-wards, outside the influence of the thick sedimentary overburden observed elsewhere.

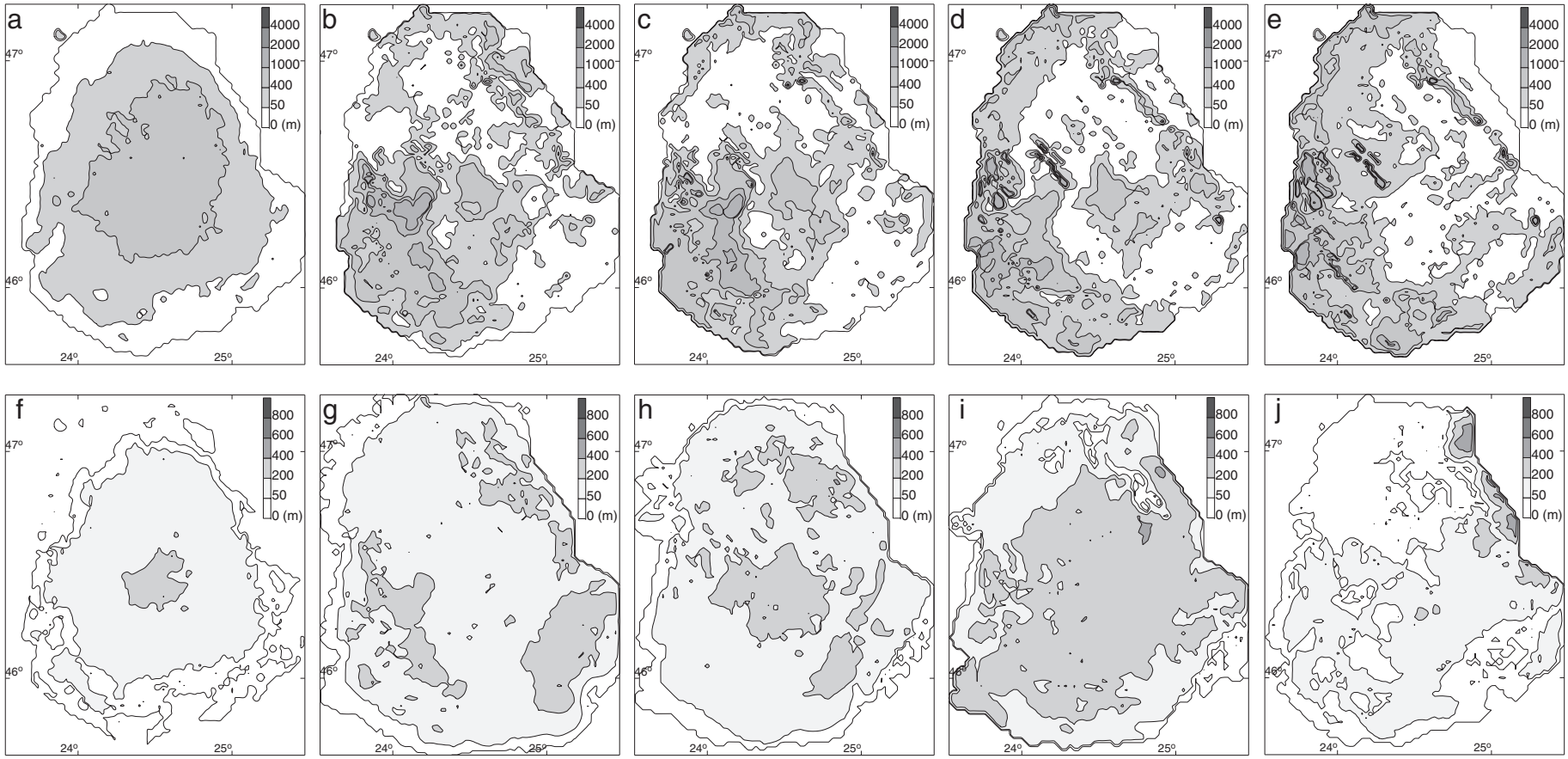

Fig. 7. Results of the computed models for salt re-distribution in the basin and tectonic subsidence by forward modelling. a) Modelled salt geometry at the end of Middle Badenian times. b) Modelled salt geometry at the end of Upper Badenian times. c) Modelled salt geometry at the end of Lower Sarmatian times. d) Modelled salt geometry at the end of Upper Sarmatian times. e) Modelled salt geometry at the end of Pannonian times. f) Modelled tectonic subsidence for Middle Badenian times. g) Modelled tectonic subsidence for Upper Badenian times. h) Modelled tectonic subsidence for Lower Sarmatian times. i) Modelled tectonic subsidence for Upper Sarmatian times. j) Modelled tectonic subsidence for Pannonian times.

The results of tectonic subsidence during Middle Badenian–Early Sarmatian in the forward model are fairly identical with the backward one, although at slightly different values. The same onset of Middle Badenian tectonic subsidence with maximum values roughly in the present day basin centre is required to accommodate the deposition of salt in the basin (Fig. 7f). Similarly with the backward scenario, the forward model predicts that the main Late Badenian tectonic subsidence is focused in particular near the SE basin and NE basin margins, but the patterns of subsidence are more regionally distributed (Fig. 7g). In the western part of the basin, the forward model indicates large amounts of Late Badenian tectonic subsidence, accommodated by lateral migration of salt. This regional pattern confirms the similar inference derived earlier by the backward modelling. During the Early Sarmatian (Fig. 7h) the subsidence has uniform values across the basin, excepting the NE and SE areas that show higher values. Comparing with the backward scenario, the forward model shows higher subsidence values, also in the centre of the basin.

As in the case of salt re-distribution, the forward model estimates different tectonic subsidence patterns during Late Sarmatian–Pannonian times when compared with the backward scenario (compare Fig. 7i, j with Fig. 6f, e, respectively). The forward model predicts an increase of tectonic subsidence during Late Sarmatian times in a depocentre located in the central–NE part of the basin (Fig. 7i). During Pannonian times the tectonic subsidence had similar rates in the entire basin (Fig. 7j), with the exception of few high values in areas located near the NE salt wall that are overprinted by local unclear patterns in the backward scenario (compare Fig. 7j with Fig. 6e). The forward modelling is not affected by erosion estimates. Therefore its predictions of smoother regional tectonic subsidence (Fig. 7i, j) suggests that these local patterns, as well as most of the small-scale local features surrounding the diapirs in the backward modelling (Fig. 6e, f) are in fact artefacts created by under-estimates of erosion.

6. Detecting the interplay between salt re-distribution and tectonic subsidence

Outside the small offset normal faults controlling the deposition of thin Badenian sediments pre-dating the evaporitic sequence (Krézsek et al., 2010), understanding the subsequent major tectonic subsidence followed by uplift of the Transylvanian Basin is rather difficult in the absence of other genetically related upper crustal structures, such as major controlling faults. The driving mechanism is generally interpreted to a variety of deep (sub-)lithospheric processes (see Tilita et al., 2013, for a detailed discussion). In this context, deriving details of tectonic subsidence evolution is important for analysing the basin mechanics. The interplay between salt re-distribution and tectonic subsidence in our dual modelling approach suggests that tectonic subsidence may be hidden by lateral migration of salt into the newly created space. Furthermore, lateral migration of salt may create significant accommodation space, even though the tectonic subsidence is non-existent or reduced. The latter feature is rather known in salt kinematic studies and can be detected usually by peripheral synclines and inverted structures, such as turtle-structure anticlines (e.g., Jackson et al., 1994).

One approach to understand the coupled salt kinematics and subsidence evolution is to combine the modelling results with seismo-stratigraphic interpretations (Fig. 8). The first order pattern of this comparison is that salt obviously migrated ultimately into present-day diapirs observed in the seismic interpretation. However, the way salt migrated in these diapirs may be observed or not by smaller scale details. The models suggest that the salt had considerable, up to 1 km thickness in the centre of the basin and migrated gradually towards its margins (centre of Fig. 8c). This initially occurred at low rates, which accelerated during Pannonian times, salt thickness decreasing to ~100 m observed presently in the central-southern part of the basin (Fig. 8d). This major migration pattern is very difficult to detect simply looking at cross-sections (Fig. 8d) or the overburden at the basin scale, even by using detailed seismic sequence stratigraphy. However, it can be detected within the syn-kinematic deposition in the rim synclines neighbouring individual diapiric structures (Fig. 8d).

A gradual growth in thickness up to the present geometry of diapirs located near the basin margins is predicted by modelling (e.g., Fig. 8a, b, km 10–20). Moreover, this indicates that salt migrated into the large-scale diapir located near the NE basin margin from both its flanks (Fig. 8a, near km 80). During the Late Badenian the sense of migration was from the basin centre towards the salt-wall at fairly low rates. This NE-wards migration continued during Late Badenian–Sarmatian times, but the reversed movement from the NE margin into the salt wall took place during the Late Sarmatian–Pannonian with increased rates. The latter process is most likely an effect of the earlier described volcanic sagging (Szakacs and Krézsek, 2006). The timing of this kinematic evolution of the salt-wall is observed by the seismo-stratigraphic interpretation through syn-kinematic deposition over both diapiric flanks, but the direction of migration cannot be clearly recognised (Fig. 8b).

The modelling suggests that the thick layer of salt was re-distributed laterally from the centre of the northern section during Late Badenian times (Fig. 8a) reaching values similar to the ones observed in the same central position southwards (Fig. 8d). However, the salt has subsequently increased in thickness in the centre of this northern section and formed the gentle diapirs presently observed, locally reaching the original depositional thickness (Fig. 8a, b). The regional pattern of changes in salt thickness is driven by the 3D salt migration, generally from south to north, but also laterally. Such patterns are fairly difficult to detect in standard 2D seismo-stratigraphic interpretation.

The central-western part of the southern section (Fig. 8c, d) is the best illustration of an apparently hidden relationship between large-scale salt migration and tectonic subsidence. The model suggests that salt was deposited in this region with reduced thicknesses of ~100 m. A rapid increase to 1 km thickness is inferred during the Late Badenian that remained roughly constant during Early Sarmatian and subsequently gradually decreased to thicknesses that were similar to the depositional ones during Late Sarmatian–Pannonian times. This increase followed by decrease to roughly the same original depositional thicknesses is in fact supported by the seismo-stratigraphic interpretation, although the modelled magnitudes of salt thickness variations may be exaggerated by the assumptions of local isostasy and hydrostatic salt response to loading. The flanks of the observed diapiric structure (Fig. 8d, around km 40) indicate a large number of Upper Badenian onlaps and thus syn-kinematic deposition that are in agreement with a coeval salt growth, while the overlying Late Sarmatian spoon-shaped gravitational collapse structure is in agreement with salt migration laterally out of this structure. The salt thickness variations are difficult to estimate by the seismo-stratigraphic model, but such variations (i.e. increase followed by decrease) in the order of 500 m can be reasonably explained.

7. The link between salt kinematics and Carpathians deformation

Previous generic studies infer that migration of salt in sedimentary basins is sensitive to local or regional deformations, though a significant change in the state of the regional intraplate stresses is required to trigger large-scale salt diapirism (e.g., Carter et al., 1993; Daudré and Cloetingh, 1994; Ismail-Zadeh et al., 2001; Jackson and Vendeville, 1994; Stephenson et al., 1992). A significant increase in the regional deformation and, therefore, state of stress took place in the Transylvanian Basin during the Middle–Late Miocene collision of the East and South Carpathians. Although deformation was rather continuous, three peak events of shortening are observed by kinematic and exhumation studies (Late Badenian, Late Sarmatian and Early Pannonian, Matenco et al., 2010; Merten et al., 2010). If intraplate stresses produced by these events have effects on the rate of salt migration in the

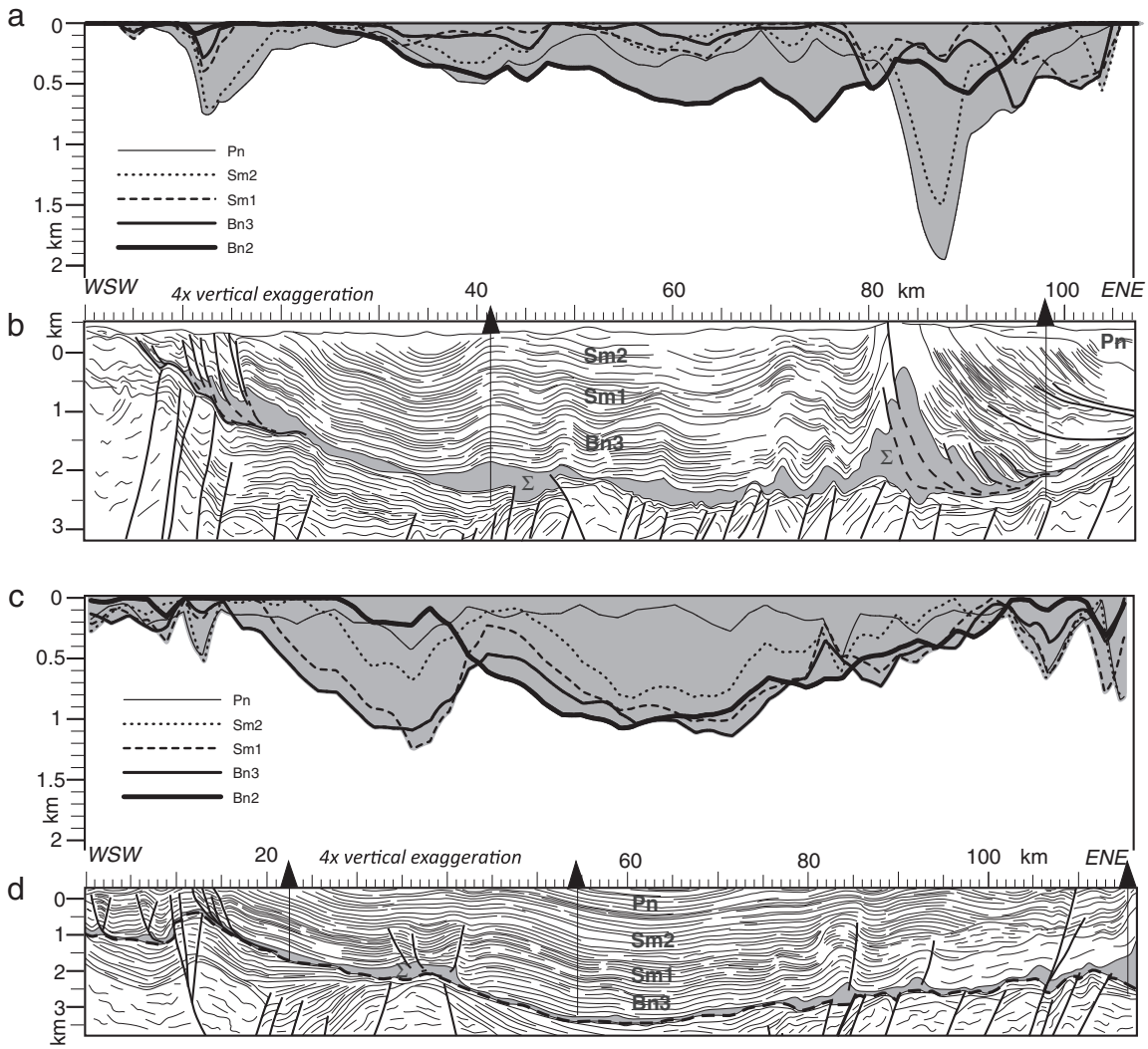

Fig. 8. Comparison between the modelled evolutions of salt in the basin during Middle–Upper Miocene times along two E–W oriented geological transects. Σ, Middle Badenian salt; Bn3, Upper Badenian; Sm1, Lower Sarmatian (i.e. Lower Volhinian); Sm2, Upper Sarmatian (i.e. Upper Volhinian–Bessarabian); Pn, Pannonian. a) and c) Predicted salt evolution by the backward model along the transects displayed in b and d, respectively; b) and d) Depth converted seismic transects crossing the basin in its northern and southern parts. Location of transects is displayed in Fig. 1. For further details on the interpretation see Tilita et al. (2013).

Transylvanian Basin, they should be visible in the backward model (e.g., Jackson and Talbot, 1986; Waltham, 1997) and in resulted differences between the backward and forward modelling of the same stratigraphic stage.

7.1. Rates of salt migration and their temporal evolution

The migration velocity is assessed using the rate of change of salt thickness in time, expressed as a first derivative of a thickness–time function (dh/dt) extracted as a best-fit spline function of the modelled thickness–time values (Fig. 9). These thickness values were extracted from the backward-modelled salt isopach grids (Fig. 6a–d). The analysis led to salt velocity curves, which were constructed for sites distributed regionally across the basin, with focus on the centre (Fig. 9b) and margins of the basin (Fig. 9c). The two main diapiric structures located in the W–SW décollement zone and in the NE salt-wall were analysed separately (Fig. 9d).

The salt migration velocity analysis infers two main evolutionary periods, i.e. Late Badenian–earliest Pannonian and the remainder of Pannonian times, which are interrupted by short phases (of 0.2–0.6 Ma) of slow salt-migration rates (Fig. 9). The first Late Badenian–earliest Pannonian period is characterised by relatively quick and abrupt velocity changes in the central part of the basin (Fig. 9b), when the salt migrated outside this area starting with the Late Badenian, reaching local peaks during Sarmatian times. The salt migrates towards the basin margins with peaks in late Badenian and late Sarmatian (Fig. 9c and d), while the salt migration rate for Early Sarmatian times displays lower and constant velocities. The second Pannonian period is characterised by low velocities of salt migration both in the basin centre and along its margins (Fig. 9b–d). These calculations indicate that the velocity of salt migration was particularly high during late Badenian–Early Pannonian times, while rather low-velocity salt movements characterised the subsequent Pannonian evolution. This is in direct agreement with the main phases of Carpathian deformation. Therefore, a direct relationship between increased velocities of salt migration and phases of Carpathian shortening is evident.

7.2. Relationship with Carpathian tectonics

The close relationship between the shortening and uplift of the surrounding Carpathians–Apuseni Mountains and the vertical movements recorded by the Transylvanian Basin has been demonstrated by a number of regional studies (Krézsek and Bally, 2006; Krézsek et al., 2010; Matenco et al., 2010; Merten et al., 2011). Our study provides a novel quantification by linking these processes with salt re-distribution inside the basin. Furthermore, this salt re-distribution

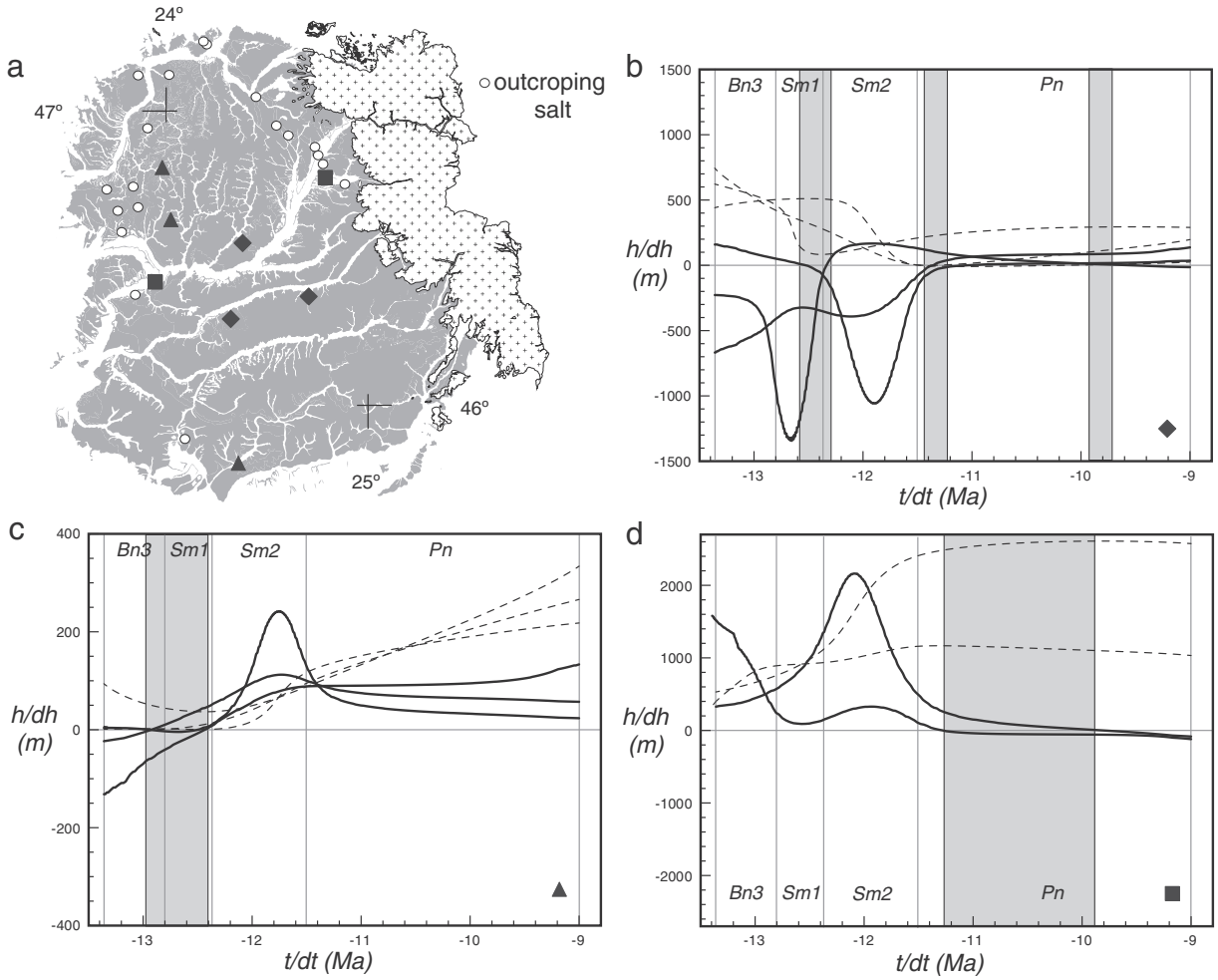

Fig. 9. Comparison of salt migration velocity within different areas of the basin. a) Sketch of the Transylvanian Basin with positions of outcropping salt areas and wells analysed. b–d) Plots of the best fit curve of thickness variation through time (thin dash black lines) and plot of the rate of thickness variation through time (thick black lines). Grey shaded areas represent periods of stagnation during salt migration. h, thickness; dh, thickness variation; t, time; dt, time variation.

masked additional components of tectonic subsidence and/or uplift that were unaccounted in existing studies.

The salt re-distribution and tectonic subsidence patterns are well predicted by forward modelling, but not their amplitudes. When compared with the backward scenario, the differences should be driven by intraplate stresses and potential errors in estimating the post-Pannonian erosion. Interestingly, the forward modelling results are significantly different from the backward approach starting with the Early Sarmatian times (compare Fig. 7h, i and j with Fig. 6g, f and e, respectively). The forward model deviates at first by slightly different patterns of coupled salt migration and tectonic subsidence in the centre of the basin, followed by a different evolution during Late Sarmatian and Pannonian times, most of the salt migrating essentially westwards. There is a clear agreement between the evolution of these differences and the observed tectonic events. While the western Apuseni Mountains remained rather stable during Miocene–Quaternary times, the East and South Carpathians accumulated 5–6 km of coeval uplift in a number of pulses (near the limit between Early and Late Sarmatian and between latest Sarmatian and Early Pannonian) that affected only the margins of the Transylvanian Basin. The end Pannonian event exhumed the entire basin to sub-aerial conditions, probably similar to the present day ones.

Alternatively, the observed difference between the forward and backward model starting with the Early Sarmatian times can also be induced by underestimating the erosion in the basin in such a way that large stratigraphic sections would have been removed in its western part, facilitating a coeval salt migration in this area. This is in disagreement with what is observed by kinematic and thermochronology studies, i.e. the relative stability of the Apuseni Mountains in the west and the coeval uplift of the East, SE and South Carpathians.

This agreement between the observed tectonic events and the moments when the forward model deviates from observations and the backward scenario indicates that the Carpathian collision has started to influence the basin by intraplate stresses starting with the Early Sarmatian. Obviously, areas affected by the short wavelength orogenic deformation are the ones close to the East and SE Carpathians. This is observed in our modelling by the different architecture of salt diapirism and tectonic subsidence in the vicinity of these mountains (Fig. 7g–h). The areas affected by the long-wavelength uplift that took place at the end of the Pannonian times are reflected by different patterns of tectonic subsidence, predicted to continue at lower rates during Pannonian period (Fig. 7j).

At larger geodynamic scale, the coupled models of salt re-distribution and tectonic subsidence can contribute to improve the understanding of Transylvanian Basin poorly constrained genesis. The forward model predicts that in the absence of Carpathians-induced intraplate stresses the tectonic subsidence of the basin (Fig. 7) would have started in Middle Badenian times and subsequently continued at high rates throughout Late Badenian–Sarmatian times, gradually decreasing during the Pannonian. The large wavelength (~200 km) of the Middle Badenian subsidence indicates a lower or sub-lithospheric mechanism, while the Late Badenian subsidence is short-wavelength and focused in a number

of much narrower areas, among which the western depocentre near the Apuseni Mountains cannot be related to the overall Carpathian deformations in the forward model. This novel observation possible demonstrates that Transylvanian Basin subsidence was driven by the extension of the Pannonian Basin, as speculatively suggested by previous studies (Matenco and Radivojević, 2012; Tilita et al., 2013). The area affected by tectonic subsidence appears to widen again during Sarmatian times, while subsequently focusing and decreasing in the centre of the basin during the Pannonian. This evolution is consistent with a dual genesis, the focused Late Badenian subsidence being overprinted by larger wavelength mechanisms acting during the entire Miocene evolution.

8. Conclusions

Our modelling of coupled tectonic subsidence and salt re-distribution has demonstrated the need of studying driving mechanisms in salt-bearing sedimentary basins located in the vicinity of convergent margins. Constrained by a detailed 3D geometry of the Transylvanian Basin derived from the interpretation of a large number of seismic lines and subsequently corrected for stratigraphic volumes, the numerical modelling of salt re-distribution and tectonic subsidence is verified with other independent seismo-stratigraphic interpretations, kinematic/exhumational studies of the neighbouring orogens and other basin studies.

The modelling shows that migration of salt inside the Transylvania Basin was far more complex than simply unidirectional. It also confirms earlier interpretations suggesting that salt migrated from the basin centre towards its margins, with the exception of the NE located area, where locally an opposite polarity migration took place due to volcanic sagging. A novel inference of the modelling is the presence of a much thicker salt sequence than previously estimated in the centre of the basin at the end of its depositional times, which implies that significant tectonic subsidence took place already during the Middle Badenian. Another novel modelling result is the presence of areas with significant tectonic subsidence hidden by the inward salt migration and areas with apparent large tectonic subsidence that are in fact artefacts of outward salt migration. Similar successive in- and out-ward salt migration events are also suggested, an effect of localised subsidence and overburden loading. All these effects are in agreement with detailed seismo-stratigraphic interpretations.

The comparison between the backward and forward modelling and the analysis of salt re-distribution rates indicates that its late Sarmatian–early Pannonian migration was accelerated by intraplate stresses created by the coeval phases of contraction recorded at the exterior of the Carpathians. This is direct evidence that salt migration is enhanced by intraplate stresses. Although speculated since a very long time (e.g., Mrazec, 1932), our study provide for the first time a quantitative link between intraplate stresses and salt diapirism in the Transylvanian Basin and confirms the generic concept of a stress-induced creation of large diapiric structures.

The numerical modelling shows for the first time that the subsidence of the Transylvanian Basin is the result of at least two superposed mechanisms, one(s) creating the long-wavelength subsidence and subsequent uplift acting at the scale of the entire basin for its entire Middle Miocene–Quaternary evolution. The other one initiated in Late Badenian is short-wavelength and had localised effects. Analysing these mechanisms require data and methodologies beyond this study, but we speculatively infer that the latter mechanism is related to the Middle Miocene peak of the extension recorded in the Pannonian Basin.

Acknowledgements

This publication is the result of the collaboration between the Netherlands Research Centre for Integrated Solid Earth Science, GFZ Potsdam, University of Bucharest and Romgaz S.A. Romgaz S.A. is acknowledged for providing geological and geophysical database from the Transylvanian Basin. Laurentiu Ionescu is acknowledged for his collaboration and continuous support. Alex Boscaneanu is thanked for his help in computing petrophysical parameters. The authors are grateful to the two anonymous reviewers for their constructive observations and suggestions that significantly improved an earlier version of this manuscript.

References

Balintoni, I., 1996. Transilvanidele vestice, comentarii structurale. Studia Universitas Babes-Bolyai Seria Geologia XLI pp. 95–100.
Beglinger, S.E., Doust, H., Cloetingh, S., 2012. Relating petroleum system and play development to basin evolution: West African South Atlantic basins. Mar. Pet. Geol. 30, 1–25.
Brun, J.-P., Fort, X., 2011. Salt tectonics at passive margins: geology versus models. Mar. Pet. Geol. 28, 1123–1145.
Buchanan, P.G., Bishop, D.J., Hood, D.N., 1996. Development of salt related structures in the Central North Sea: results from section balancing. In: Alsop, G.I., Blundell, D.J., Davison, I. (Eds.), Salt Tectonics. Geological Society Special Publication 100, pp. 111–128.
Carter, N.L., Horseman, S.T., Russelland, J.E., Handin, J., 1993. Rheology of rocksalt. J. Struct. Geol. 15, 1257–1271.
Ciulavu, D., 1999. Tertiary tectonics of the Transylvanian Basin (PhD Thesis), Vrije Universiteit, Amsterdam (152 pp.).
Ciulavu, D., Dinu, C., Szakacs, A., Dordea, D., 2000. Late Miocene to Pliocene kinematics of the Transylvania basin. Am. Assoc. Pet. Geol. Bull. 84, 1589–1615.
Ciupagea, D., Paucă, M., Ichim, T., 1970. Geologia bazinului Transilvaniei (in Romanian). Editura Tehnica, Bucuresti.
Cloetingh, S.A.P.L., Burov, E., Matenco, L., Toussaint, G., Bertotti, G., Andriessen, P.A.M., Wortel, M.J.R., Spakman, W., 2004. Thermo-mechanical controls on the mode of continental collision in the SE Carpathians (Romania). Earth Planet. Sci. Lett. 218, 57–76.
Cloetingh, S., Matenco, L., Bada, G., Dinu, C., Mocanu, V., 2005. The evolution of the Carpathians–Pannonian system: interaction between neotectonics, deep structure, polyphase orogeny and sedimentary basins in a source to sink natural laboratory. Tectonophysics 410, 1–14.
Cloetingh, S.A.P.L., Van Wees, J.D., Ziegler, P.A., Lenkey, L., Beekman, F., Tesauro, M., Förster, A., Norden, B., Kaban, M., Hardebol, N., Bonté, D., Genter, A., Guillou-Frottier, L., Ter Voorde, M., Sokoutis, D., Willingshofer, E., Cornu, T., Worum, G., 2010. Lithosphere tectonics and thermo-mechanical properties: an integrated modelling approach for Enhanced Geothermal Systems exploration in Europe. Earth Sci. Rev. 102, 159–206.
Cloetingh, S., Burov, E., Matenco, L., Beekman, F., Roure, F., Ziegler, P.A., 2013. The Moho in extensional tectonic settings: insights from thermo-mechanical models. Tectonophysics 609, 558–604.
Corver, M.P., Doust, H., van Wees, J.D., Cloetingh, S., 2011. Source-rock maturation characteristics of symmetric and asymmetric grabens inferred from integrated analogue and numerical modelling: the southern Viking Graben (North Sea). Mar. Pet. Geol. 28, 921–935.
Cranganu, C., Deming, D., 1996. Heat flow and hydrocarbon generation in the Transylvanian Basin, Romania. Am. Assoc. Pet. Geol. Bull. 80, 1641–1653.
Csontos, L., Nagymarosy, A., 1998. The Mid-Hungarian line: a zone of repeated tectonic inversions. Tectonophysics 297, 51–71.
Csontos, L., Vörös, A., 2004. Mesozoic plate tectonic reconstruction of the Carpathian region. Palaeogeogr. Palaeoclimatol. Palaeoecol. 210, 1–56.
Daudré, B., Cloetingh, S., 1994. Numerical modelling of salt diapirism: influence of the tectonic regime. Tectonophysics 240, 59–79.
Davison, I., Alsop, G.I., Blundell, D.J., 1995. Salt tectonics: some aspects of deformation mechanics. In: Alsop, G.I., Blundell, D.J., Davison, I. (Eds.), Salt Tectonics. Geological Society, London, Special Publication 100, pp. 1–10.
De Broucker, G., Mellin, A., Duindam, P., 1998. Tectono-stratigraphic evolution of the Transylvanian basin, pre-salt sequence, Romania. In: Dinu, C., Mocanu, V. (Eds.), Geological structure and hydrocarbon potential of the Romanian areas, Bucharest Geoscience Forum Special volume no. 1, Bucharest, pp. 36–69.
de Leeuw, A., Bukowski, K., Krijgsman, W., Kuiper, K.F., 2010. Age of the Badenian salinity crisis; impact of Miocene climate variability on the circum-Mediterranean region. Geology 38, 715–718.
de Leeuw, A., Filipescu, S., Matenco, L., Krijgsman, W., Kuiper, K., Stoica, M., 2013. Paleomagnetic and chronostratigraphic constraints on the Middle to Late Miocene evolution of the Transylvanian Basin (Romania): implications for Central Paratethys stratigraphy and emplacement of the Tisza–Dacia plate. Glob. Planet. Chang. 103, 82–98.
Diehl, J.F., Beck Jr., M.E., Beske-Diehl, S., Jacobson, D., Hearn Jr., B.C., 1983. Paleomagnetism of the Late-Cretaceous-early Tertiary north-central Montana alkalic province. J. Geophys. Res. 88, 10593–10609.
Filipescu, S., Gîrbacea, R., 1997. Lower Badenian sea-level drop on the western border of the Transylvanian basin: foraminiferal paleobathymetry and stratigraphy. Geol. Carpath. 48, 325–334.
Ghergari, L., Meszaros, N., Hosu, A., Filipescu, S., Chira, C., 1991. The gypsiferous formation at Cheia (Cluj County). Studia Universitas Babes-Bolyai Seria Geologia Cluj Napoca 36 pp. 13–28.
Graham, R., Jackson, M., Pilcher, R., Kilsdonk, B., 2012. Allochthonous salt in the sub-Alpine fold–thrust belt of Haute Provence, France. Geol. Soc. Lond., Spec. Publ. 363, 595–615.

Haas, J., Péró, C., 2004. Mesozoic evolution of the Tisza Mega-unit. Int. J. Earth Sci. 93, 297–313.
Hecht, C.A., Lempp, C., Scheck, M., 2003. Geomechanical model for the post-Variscan evolution of the Permocarboniferous-Mesozoic basins in Northeast Germany. Tectonophysics 373, 125–139.
Hoeck, V., Ionescu, C., Balintoni, I., Koller, F., 2009. The Eastern Carpathians "ophiolites" (Romania): remnants of a Triassic ocean. Lithos 108, 151–171.
Horváth, F., Bada, G., Szafian, P., Tari, G., Adam, A., Cloetingh, S., 2006. Formation and deformation of the Pannonian Basin: constraints from observational data. Geol. Soc. Lond. Mem. 32, 191–206.
Iancu, V., Berza, T., Seghedi, A., Gheuca, I., Hann, H.-P., 2005. Alpine polyphase tectono-metamorphic evolution of the South Carpathians: a new overview. Tectonophysics 410, 337–365.
Ionescu, C., Hoeck, V., Tomek, C., Koller, F., Balintoni, I., Besutiu, L., 2009. New insights into the basement of the Transylvanian Depression (Romania). Lithos 108, 172–191.
Ismail-Zadeh, A.T., Talbot, C.J., Volozh, Y.A., 2001. Dynamic restoration of profiles across diapiric structures: numerical approach and its applications. Tectonophysics 337, 23–38.
Ismail-Zadeh, A., Tsepelev, I., Talbot, C., Korotkii, A., 2004. Three-dimensional forward and backward modelling of diapirism: numerical approach and its applicability to the evolution of salt structures in the Precaspian basin. Tectonophysics 387, 81–103.
Ismail-Zadeh, A., Maţenco, L., Radulian, M., Cloetingh, S., Panza, G., 2012. Geodynamics and intermediate-depth seismicity in Vrancea (the south-eastern Carpathians): current state-of-the art. Tectonophysics 530–531, 50–79.
Jackson, M.P.A., Talbot, C.J., 1986. External shapes, strain rates, and dynamics of salt structures. Geol. Soc. Am. Bull. 97, 305–323.
Jackson, M.P.A., Vendeville, B.C., 1994. Regional extension as a geological trigger for diapirism. Geol. Soc. Am. Bull. 106, 57–73.
Jackson, M., Vendeville, B.C., Schultz-Ela, D.D., 1994. Structural dynamics of salt systems. Annu. Rev. Earth Planet. Sci. 22, 93–117.
Jenyon, M.K., 1986. Salt Tectonics. Elsevier Applied Science, p. 192.
Kounov, A., Schmid, S., 2013. Fission-track constraints on the thermal and tectonic evolution of the Apuseni Mountains (Romania). Int. J. Earth Sci. 102, 207–233.
Koyi, H., Talbot, C.J., Tørudbakken, B.O., 1993. Salt diapirs of the southwest Nordkapp Basin: analogue modelling. Tectonophysics 228, 167–187.
Krézsek, C., Bally, A.W., 2006. The Transylvanian Basin (Romania) and its relation to the Carpathian fold and thrust belt: insights in gravitational salt tectonics. Mar. Pet. Geol. 23, 405–442.
Krézsek, C., Filipescu, S., 2005. Middle to late Miocene sequence stratigraphy of the Transylvanian Basin (Romania). Tectonophysics 410, 437–463.
Krézsek, C., Adam, J., Grujic, D., 2007. Mechanics of fault and expulsion rollover systems developed on passive margins detached on salt: insights from analogue modelling and optical strain monitoring. Geol. Soc. Lond., Spec. Publ. 292, 103–121.
Krézsek, C., Filipescu, S., Silye, L., Matenco, L., Doust, H., 2010. Miocene facies associations and sedimentary evolution of the Southern Transylvanian Basin (Romania): implications for hydrocarbon exploration. Mar. Pet. Geol. 27, 191–214.
Krézsek, C., Lapadat, A., Matenco, L., Arnberger, K., Barbu, V., Olaru, R., 2013. Strain partitioning at orogenic contacts during rotation, strike-slip and oblique convergence: Paleogene–Early Miocene evolution of the contact between the South Carpathians and Moesia. Glob. Planet. Chang. 103, 63–81.
Magyar, I., Geary, D.H., Muller, P., 1999. Paleogeographic evolution of the Late Miocene Lake Pannon in Central Europe. Palaeogeogr. Palaeoclimatol. Palaeoecol. 147, 151–167.
Martin, M., Wenzel, F., CALIXTO Group, 2006. High-resolution teleseismic body wave tomography beneath SE-Romania: II. Imaging of a slab detachment scenario. Geophys. J. Int. 164, 579–595.
Mason, P.R.D., Seghedi, I., Szakacs, A., Downes, H., 1998. Magmatic constraints on geodynamic models of subduction in the East Carpathians, Romania. Tectonophysics 297, 157–176.
Matenco, L., Andriessen, P., 2013. Quantifying the mass transfer from mountain ranges to deposition in sedimentary basins: source to sink studies in the Danube Basin–Black Sea system. Glob. Planet. Chang. 103, 1–18.
Matenco, L., Radivojević, D., 2012. On the formation and evolution of the Pannonian Basin: constraints derived from the structure of the junction area between the Carpathians and Dinarides. Tectonics 31, TC6007. http://dx.doi.org/10.1029/2012tc003206.
Matenco, L., Bertotti, G., Leever, K., Cloetingh, S., Schmid, S., Tărăpoancă, M., Dinu, C., 2007. Large-scale deformation in a locked collisional boundary: interplay between subsidence and uplift, intraplate stress, and inherited lithospheric structure in the late stage of the SE Carpathians evolution. Tectonics 26, TC4011. http://dx.doi.org/10.1029/2006TC001951.
Matenco, L., Krézsek, C., Merten, S., Schmid, S., Cloetingh, S., Andriessen, P., 2010. Characteristics of collisional orogens with low topographic build-up: an example from the Carpathians. Terra Nova 22, 155–165.
Maystrenko, Y., Bayer, U., Scheck-Wenderoth, M., 2006. 3D reconstruction of salt movements within the deepest post-Permian structure of the Central European Basin System–the Glueckstadt Graben. Neth. J. Geosci, - Geol. Mijnb. 85, 181–196.
Maystrenko, Y.P., Bayer, U., Scheck-Wenderoth, M., 2013. Salt as a 3D element in structural modelling—example from the Central European Basin System. Tectonophysics 591, 62–82.
McClay, K.R., Whitehouse, P.S., Dooley, T., Richards, A., 2004. 3D evolution of fold and thrust belts formed by oblique convergence. Mar. Pet. Geol. 21, 857–877.
Merten, S., Matenco, L., Foeken, J.P.T., Stuart, F.M., Andriessen, P.A.M., 2010. From nappe stacking to out-of-sequence postcollisional deformations: Cretaceous to Quaternary exhumation history of the SE Carpathians assessed by low-temperature thermochronology. Tectonics 29, TC3013.
Merten, S., Matenco, L., Foeken, J.P.T., Andriessen, P.A.M., 2011. Toward understanding the post-collisional evolution of an orogen influenced by convergence at adjacent plate margins: Late Cretaceous–Tertiary thermotectonic history of the Apuseni Mountains. Tectonics 30, TC6008. http://dx.doi.org/10.1029/2011tc002887.
Morley, C.K., 1996. Models for relative motion of crustal blocks within the Carpathian region, based on restorations of the outer Carpathian thrust sheets. Tectonics 15, 885–904.
Mrazec, L., 1932. Considerations sur l'origine des depressions internes des Carpates Roumaines. Bul. Soc. Rom. Geol. 1, 115–125.
Nagihara, S., Sclater, J.G., Beckley, L.M., Behrens, E.W., Lawver, L.A., 1992. High heat flow anomalies over salt structures on the Texas continental slope, Gulf of Mexico. Geophys. Res. Lett. 19, 1687–1690.
Nalpas, T., Brun, J.P., 1993. Salt flow and diapirism related to extension at crustal scale. Tectonophysics 228, 349–362.
Nicolae, I., Saccani, E., 2003. Petrology and geochemistry of the Late Jurassic calc-alkaline series associated to Middle Jurassic ophiolites in the South Apuseni Mountains (Romania). Schweiz. Mineral. Petrogr. Mitt. 83, 81–96.
Oncescu, M.C., Bonjer, K.P., 1997. A note on the depth recurrence and strain release of large Vrancea earthquakes. Tectonophysics 272, 291–302.
Paraschiv, D., 1997. The pre-Paratethys buried denudational surface in Romanian territory. Rev. Roum. Géogr. 41, 21–32.
Paucă, M., 1968. Problemes tectoniques dans le Bassin de Transylvanie. Geol. Rundsch. 58, 520–537.
Pecskay, Z., Lexa, J., Szakacs, A., Balogh, K., Seghedi, I., Konecny, V., Kovacs, M., Marton, M., Kaliciak, M., Szeky- Fux, V., Poka, T., Gyarmaty, P., Edelstein, O., Rosu, E., Zec, B., 1995. Space and time distribution of Neogene–Quaternary volcanism in the Carpatho–Pannonian region. Acta Volcanol. 7, 15–29.
Peryt, T.M., 2006. The beginning, development and termination of the Middle Miocene Badenian salinity crisis in Central Paratethys. Sediment. Geol. 188–189, 379–396.
Petersen, K., Lerche, I., 1995. Quantification of thermal anomalies in sediments around salt structures. Geothermics 24, 253–268.
Podlachikov, Y., Talbot, C., Poliakov, A.N.B., 1993. Numerical models of complex diapirs. Tectonophysics 228, 189–198.
Poliakov, A.N.B., Podlachikov, Y., Talbot, C., 1993. Initiation of salt diapirs with frictional overburdens: numerical experiments. Tectonophysics 228, 199–210.
Răbăgia, T., Matenco, L., Cloetingh, S., 2011. The interplay between eustacy, tectonics and surface processes during the growth of a fault-related structure as derived from sequence stratigraphy: the Govora–Ocnele Mari antiform, South Carpathians. Tectonophysics 502, 196–220.
Rădulescu, F., 1988. Seismic models of the crustal structure in Romania. Rev. Roum. Géol. Géophys. Géogr. Sér. Géophys. 32, 13–17.
Robertson, A., Karamata, S., Saric, K., 2009. Overview of ophiolites and related units in the Late Palaeozoic–Early Cenozoic magmatic and tectonic development of Tethys in the northern part of the Balkan region. Lithos 108, 1–36.
Rögl, F., 1999. Mediteranean and Paratethys. Facts and hypotheses of an Oligocene to Miocene paleogeography. Geol. Carpath. 50, 339–349.
Roure, F., 2008. Foreland and Hinterland basins: what controls their evolution? Swiss J. Geosci. 101, 5–29.
Roure, F., Roca, E., Sassi, W., 1993. The Neogene evolution of the outer Carpathian flysch units (Poland, Ukraine and Romania); kinematics of a foreland/ fold-and-thrust belt system. Sediment. Geol. 86, 177–201.
Rowan, M.G., 1993. A systematique technique for the sequential restoration of salt structures. Tectonophysics 228, 331–348.
Rowan, M.G., Ratliff, R.A., 2012. Cross-section restoration of salt-related deformation: Best practices and potential pitfalls. J. Struct. Geol. 41, 24–37.
Săndulescu, M., 1988. Cenozoic Tectonic History of the Carpathians. In: Royden, L.H., Horváth, F. (Eds.), The Pannonian Basin, a study in basin evolution. American Association of Petroleum Geologists Memoir 45, pp. 17–25.
Săndulescu, M., Visarion, M., 1977. Considerations sur la structure tectonique du soubassement de la depression de Transylvanie. Dari de seama ale sedintelor, Institutul de Geologie si Geofizica LXIV pp. 153–173.
Săndulescu, M., Visarion, M., 1988. La structure des plate-formes situées dans l´avant-pays et au-dessous des nappes du flysch des Carpathes orientales. Studii tehnice si economice, Seria Geofizica 15 pp. 62–67.
Schäfer, F., Griffiths, P., Osborn, R., 1998. Balancing salt structures in 3D. Tagungsband zum 18. DGMK-Mintrop-Seminar. Ruhr-Universitat Bochum, pp. 69–107.
Scheck, M., Bayer, U., 1999. Evolution of the northeast German basin—inferences from a 3D structural model and subsidence analysis. Tectonophysics 313, 145–169.
Scheck, M., Bayer, U., Lewerenz, B., 2003. Salt movements in the Northeast German Basin and its relation to major post-Permian tectonic phases–results from 3D structural modelling, backstripping and reflection seismic data. Tectonophysics 361, 277–299.
Schmid, S., Bernoulli, D., Fügenschuh, B., Matenco, L., Schefer, S., Schuster, R., Tischler, M., Ustaszewski, K., 2008. The Alpine–Carpathian–Dinaridic orogenic system: correlation and evolution of tectonic units. Swiss J. Geosci. 101, 139–183.
Schultz-Ela, D., Jackson, M.P.A., Vendeville, B., 1993. Mechanics of active salt diapirism. Tectonophysics 228, 275–312.
Seghedi, I., Szakacs, A., 1991. The Dej tuff from Dej-Ciceu area: some petrographical, petrochemical and volcanological aspects. In: Bedelean, I., Ghergari, L., Marza, I., Meszaros, N., Nicorici, E., Petrescu, I. (Eds.), The Volcanic Tuffs from the Transylvanian Basin, Romania. University of Cluj Napoca, Cluj Napoca, pp. 135–146.
Seghedi, I., Downes, H., Szakacs, A., Mason, P.R.D., Thirlwall, M.F., Rosu, E., Pecskay, Z., Marton, E., Panaiotu, C., 2004. Neogene–Quaternary magmatism and geodynamics in the Carpathian–Pannonian region: a synthesis. Lithos 72, 117–146.
Senes, J., 1973. Correlation hypotheses of the Neogene Tethys and Paratethys. Giorn. Geol. 39, 271–286.
Smit, J.H.W., Brun, J.P., Sokoutis, D., 2003. Deformation of brittle-ductile thrust wedges in experiments and nature. J. Geophys. Res. 108, 2480. http://dx.doi.org/10.1029/2002JB002190.

Smit, J., Brun, J.P., Fort, X., Cloetingh, S., Ben-Avraham, Z., 2008. Salt tectonics in pull-apart basins with application to the Dead Sea Basin. Tectonophysics 449, 1–16.
Steininger, F.F., Muller, C., Rogl, F., 1988. Correlation of Central Paratethys, Eastern Paratethys, and Mediterranean Neogene Stages. In: Royden, L.H., Horváth, F. (Eds.), The Pannonian Basin, A Study in Basin Evolution. American Association of Petroleum Geologists Memoir 28, pp. 79–87.
Stephenson, R.A., van Berkel, J.T., Cloetingh, S.A.P.L., 1992. Relation between salt diapirism and the tectonic history of the Sverdrup Basin, Arctic Canada. Can. J. Earth Sci. 29, 2695–2705.
Stewart, S.A., Harvey, M.J., Otto, S.C., Weston, P.J., 1996. Influence of salt on fault geometry: examples from the UK salt basins. In: Alsop, G.I., Blundell, D.J., Davison, I. (Eds.), Salt Tectonics. Geological Society, London, Special Publication 100, pp. 175–202.
Szabo, C., Harangi, S., Csontos, L., 1992. Review of Neogene and Quaternary volcanism of the Carpathian-Pannonian region. Tectonophysics 208, 243–256.
Szakacs, A., Krézsek, C., 2006. Volcano-basement interaction in the Eastern Carpathians: explaining unusual tectonic features in the Eastern Transylvanian Basin, Romania. J. Volcanol. Geotherm. Res. 158, 6–20.
Sztanó, O., Krézsek, C., Magyar, I., Wanek, F., Juhász, G., 2005. Sedimentary cycles and rhythms in a Sarmatian to Pannonian (Late Miocene) transitional section at Oarba de Mures/Marosorbó, Transylvanian Basin. Acta Geol. Hung. 48, 235–257.
ter Borgh, M., Vasiliev, I., Stoica, M., Knežević, S., Matenco, I., Krijgsman, W., Rundić, L., Cloetingh, S., 2013. The isolation of the Pannonian basin (Central Paratethys): new constraints from magnetostratigraphy and biostratigraphy. Glob. Planet. Chang. 103, 99–118.
Thomsen, R.O., Lerche, I., 1991. Salt diapir velocity assessment from temperature and thermal indicator anomalies: application to Lulu-1, Danish North Sea. Terra Nova 3, 500–509.
Tilita, M., Matenco, L., Dinu, C., Ionescu, L., Cloetingh, S., 2013. Understanding the kinematic evolution and genesis of a back-arc continental "sag" basin: the Neogene evolution of the Transylvanian Basin. Tectonophysics 602, 237–258.
Tischler, M., Gröger, H.R., Fügenschuh, B., Schmid, S.M., 2007. Miocene tectonics of the Maramures area (Northern Romania): implications for the Mid-Hungarian fault zone. Int. J. Earth Sci. 96, 473–496. http://dx.doi.org/10.1007/s00531-00006-00110-x.
Tischler, M., Matenco, L., Filipescu, S., Groger, H.R., Wetzel, A., Fugenschuh, B., 2008. Tectonics and sedimentation during convergence of the ALCAPA and Tisza-Dacia continental blocks: the Pienide nappe emplacement and its foredeep (N. Romania). Geol. Soc. Lond., Spec. Publ. 298, 317–334.
Ustaszewski, K., Schmid, S., Fügenschuh, B., Tischler, M., Kissling, E., Spakman, W., 2008. A map-view restoration of the Alpine–Carpathian–Dinaridic system for the Early Miocene. Swiss J. Geosci. 101, 273–294.
van der Hoeven, A.G.A., Mocanu, V., Spakman, W., Nutto, M., Nuckelt, A., Matenco, L., Munteanu, L., Marcu, C., Ambrosius, B.A.C., 2005. Observation of present-day tectonic motions in the southeastern Carpathians: results of the ISES/CRC-461 GPS measurements. Earth Planet. Sci. Lett. 239, 177–184. http://dx.doi.org/10.1016/j.epsl.2005.09.018.
van Keken, P.E., Spiers, C.J., Van den Berg, A.P., Muyzert, E.J., 1993. The effective viscosity of rocksalt: implementation of steady-state creep laws in numerical models of salt diapirism. Tectonophysics 225, 457–476.
van Wees, J.D., Beekman, F., 2000. Lithosphere rheology during intraplate basin extension and inversion: inferences from automated modelling of four basins in western Europe. Tectonophysics 320, 219–242.
Vendeville, B.C., Jackson, M.P.A., 1992. The Rise of diapirs during thin-skinned extension. Mar. Pet. Geol. 9, 331–353.
Vendeville, B.C., Hongxing, G., Jackson, M.P.A., 1995. Scale models of salt tectonics during basement-involved extension. Pet. Geosci. 1, 179–183.
Visarion, M., Săndulescu, M., Stănica, D., Veliciu, S., 1988. Contributions á la connaissance de la structure profonde de la plate-forme Moésienne en Roumanie. Studii tehnice economice, Seria Geofizica 15 pp. 68–92.
Waltham, D., 1997. Why does salt start to move? Tectonophysics 282, 117–128.
Warsitzka, M., Kley, J., Kukowski, N., 2013. Salt diapirism driven by differential loading—some insights from analogue modelling. Tectonophysics 591, 83–97.
Whitefield, C., Jaffri, F., Griffiths, P.A., Jones, S., 1999. 3D computer modelling and restoration of Gulf of Mexico-type allochtonous salt structures. American Association of Petroleum Geologists, 1999 Annual Meeting, Annual Meeting Expanded Abstracts. American Association of Petroleum Geologists, San Antonio, TX, p. A150.
Yin, H., Groshong Jr., R.H., 1999. Salt piercement structures, 3-D kinematic modelling and balanced cross-sections; preliminary results. Geological Society of America, 1999 Annual Meeting, Abstracts with Programs vol. 31; 7. Geological Society of America, San Antonio, TX, p. 126.
Zirngast, M., 1996. The development of the Gorleben salt dome (northwest Germany) based on quantitative analysis of peripheral sinks. In: Alsop, G.I., Blundell, D.J., Davison, I. (Eds.), Salt Tectonics. Geological Society, London, Special Publication 100, pp. 203–226.